UNPUBLISHED PRELIMINARY DATA

Department of AERONAUTICS and ASTRONAUTICS
STANFORD UNIVERSITY

115 p.

A. CRAIG
AND
I. FLÜGGE-LOTZ

N64 13189
CODE-1
NASA CR 55.149

REALIZATION OF MINIMUM CONTROL-EFFORT OPTIMAL CONTROL

OTS PRICE

XEROX $ 9.60 ph.

MICROFILM $ 3.65 mf.

RESEARCH SPONSORED BY THE NATIONAL AERONAUTICS AND SPACE ADMINISTRATION
UNDER GRANT NsG 133-61
AND BY THE AIR FORCE OFFICE OF SCIENTIFIC RESEARCH UNDER GRANTS
AF-AFOSR-137-63 AND AF-AFOSR-235-63

OCTOBER
1963

SUDAER
NO. 171

Department of Aeronautics and Astronautics
Stanford University
Stanford, California

REALIZATION OF MINIMUM CONTROL EFFORT OPTIMAL CONTROL

by

Andrew Craig
and
Irmgard Flügge-Lotz

SUDAER No. 171
October 1963

ABSTRACT

13189

Application of Pontryagin's Optimal Principle to control system problems eventually requires that a two-point boundary value problem be solved. For plants whose equations of motion are greater than second order this represents a formidable barrier in realizing a practical feedback control. When the criterion for optimization is minimum fuel consumption, choice of time for solution may be used as a free parameter, and this plus consideration of the efficiency of application of control leads to an approximate method which avoids this difficulty.

A heuristic analysis of the geometry of state-space trajectories, using true optimal solutions as a guide, provides laws for constructing a feedback control from the state variables. It further provides a knowledge of the bounds of performance of the mechanized sub-optimal control and an estimate on the performance of a minimum time control for comparison purposes.

As examples, the method is applied to minimum fuel control of second-order systems whose transfer functions are $1/s^2$, $1/(s^2+1)$, and $1/(s^2+2\zeta s+1)$. A more complex example of the attitude control of an earth-orbiting satellite is also given, representing a fourth-order system with two controls.

AUTHOR

$$\omega_2/\omega_1 \leq 10 \qquad \omega_2 > \omega_1$$

The task is now to select u_1 and u_2 so as to maintain $\underline{X}$ at a desired state, and to use the least control fuel in doing so.

Omitting terms which do not include $\underline{u}$ in the Hamiltonian, the function to be maximized for this system is

$$H^* = \underline{p}^T D\underline{u} - |u_1| - |u_2| \tag{45}$$

and substitution of the components of $\underline{p}^T$ and D yields

$$\begin{aligned} \max H^* &= \max\left[(p_2 + \beta_2 p_3)u_1 + (\beta_1 p_1 + p_4)u_2 - |u_1| - |u_2|\right] \\ &= f_1 u_1 - |u_1| + f_2 u_2 - |u_2| \end{aligned} \tag{46}$$

The control law, following Eq. (8), is

$$\begin{aligned} u_1 &= U_1 \operatorname{sgn} f_1 \quad , \text{ if } \quad U_1|f_1| \geq U_1 \\ &= 0 \quad , \text{ if } \quad U_1|f_1| < U_1 \\ u_2 &= U_2 \operatorname{sgn} f_2 \quad , \text{ if } \quad U_2|f_2| \geq U_2 \\ &= 0 \quad , \text{ if } \quad U_2|f_2| < U_2 \end{aligned} \tag{47}$$

By using the adjoint equation expanded into components, the functions f_1 and f_2 can be written explicitly as functions of time. The differential equations for the adjoints are

$$p_1 = \overset{o}{p}_2 (-1/\omega_1)$$

$$\overset{oo}{p}_2 + \omega_1^2 p_2 = 0 \tag{48}$$

and

$$p_3 = \overset{o}{p}_4 (-1/\omega_2)$$

$$\overset{oo}{p}_4 + \omega_2^2 p_4 = 0$$

The p_i are harmonic functions of time. By employing maximum amplitude P_i and phase angle as constants in the solution for p_i, the functions f_1 and f_2 can be written

$$f_1 = P_2 \cos(\omega_1 \tau + \delta_1) + \beta_2 P_4 \sin(\omega_2 \tau + \delta_2)$$

$$f_2 = P_4 \cos(\omega_2 \tau + \delta_2) + \beta_1 P_2 \sin(\omega_1 \tau + \delta_1) \tag{49}$$

A plot of a coast function trajectory both in a f_1 versus f_2 plane and as time histories of f_1 and f_2 are presented in Fig. 17 to illustrate an arbitrary problem.

1. Choice of Time for Solution for the Fourth-Order System

To learn how variations of T affect the problem, an analytic investigation might be made, seeking solutions to the system equations for a range

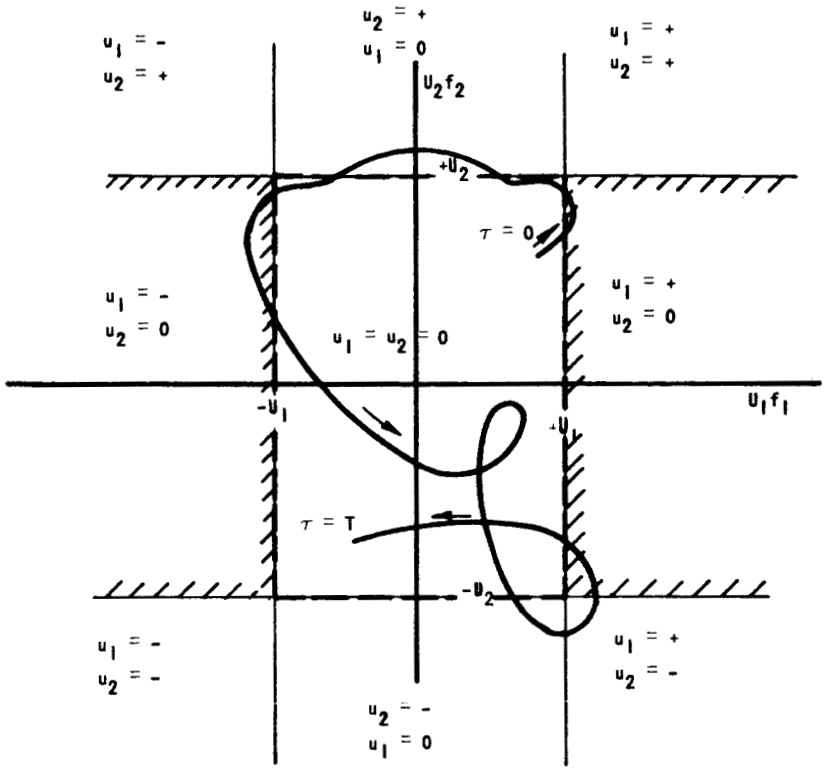

a. Sketch of the Function $f_2(f_1)$ for Visualization of Control Action.

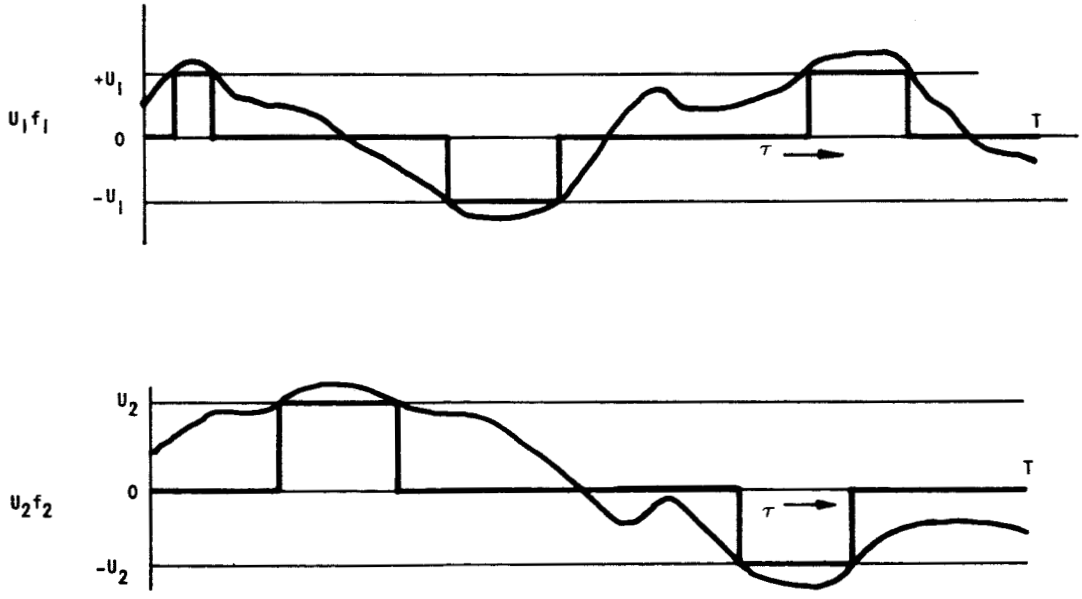

b. Control Time History.

FIG. 17. CONTROL LAW TRAJECTORIES.

of values of T and a given $\underline{X}(0)$. Inspection of the equations, particularly the control law (Eq. (47)), tends to discourage this method since in general f_1 and f_2 are aperiodic with four parameters to match to a corresponding $\underline{X}(0)$. Also, the properties sought, like a simple control law may not have a simple form in the mathematical expressions and thus go unrecognized. However, if a family of solutions could be found, a comparison of the state-space trajectories would show how T influences location of control switching points, mixing of the two controls, and the overall character of the solutions. One approach would be to let an analog computer deal with the mathematics, translating the equations into visible behavior. The adjoint system could be mechanized, a control constructed as a function of the adjoint variables in accordance with the control law, and the control applied to a synthesis of the plant. Further, to guarantee ending up at the proper value of $\underline{X}(T)$ - namely zero - the simulation can be made to operate in backward time (let $\tau^* = T - \tau$). Now the trajectory commences at the origin of $\underline{X}$ space and is driven outward by the control to pass through the point corresponding to $\underline{X}(0)$ in forward time, which is $\underline{X}(T)$ in backward time. If a family of curves can be passed through this point, the uniqueness* of optimal solutions assures that a family of different values of T were used.

Forcing solutions to pass through a particular point in a four-dimensional space is not necessarily trivial, but the cause is aided by two factors: first, the four-space in this problem can be decomposed into two two-dimensional

---

*Some plants have non-unique solutions in this respect. For example, the $1/s^2$ plant dealt with in the previous section can have the same value of F for several values of T and different trajectories for a given F and T (Ref. 7). The oscillatory plant solutions are unique.

spaces related only in time, and second, a feature of modern analog computation called repetitive operation greatly speeds up the process. In repetitive operation, the computer essentially solves the problem many times per second. When these solutions are displayed on an oscilloscope, they appear continuous and a graphic picture of the effect of parameter changes is obtained. In this manner, a parameter surface can be searched rapidly to find the desired solution: in this case, the components of $\underline{p}(0)$ were varied to satisfy a condition in $\underline{X}$.

A block diagram of such a simulation is given in Appendix E.

Some clues as to the behavior of the solutions might be obtained prior to the simulation by studying the geometry of trajectories in state space.

2. Uses of Phase Plane Geometry

The solutions of the system equations (43) can be combined to eliminate time, yielding for an interval between switchings ($\overset{o}{u}_1 = 0$, $\overset{o}{u}_2 = 0$)

$$\left[X_1(0) - \frac{U_1}{\omega_1}\right]^2 + \left[X_2(0) + \frac{\beta_1 U_2}{\omega_1}\right]^2 = \left[X_1 - \frac{U_1}{\omega_1}\right]^2 + \left[X_2 + \frac{\beta_1 U_2}{\omega_1}\right]^2$$
$$\left[X_3(0) - \frac{U_2}{\omega_2}\right]^2 + \left[X_4(0) + \frac{\beta_2 U_1}{\omega_2}\right]^2 = \left[X_3 - \frac{U_2}{\omega_2}\right]^2 + \left[X_4 + \frac{\beta_2 U_1}{\omega_2}\right]^2 \qquad (50)$$

These are equations of circles whose centers are at points determined by the control being applied. Since there are three possibilities for u_1 and three for u_2, at any instant of time the trajectories in both the X_1X_2 plane and the X_3X_4 plane are portions of circles about one of nine points in each plane. Combinations are tabulated below and plotted in Fig. 18.

Symbol	u_1	u_2	Center in X_1X_2 Plane	Center in X_3X_4 Plane
▲	+	+	$X_1 = \frac{U_1}{\omega_1}$, $X_2 = \frac{-\beta_1 U_2}{\omega_1}$	$X_3 = \frac{U_2}{\omega_2}$, $X_4 = \frac{-\beta_2 U_1}{\omega_2}$
⊛	+	0	$= 0$	$= 0$
◆	+	-	$= \frac{+\beta_1 U_2}{\omega_1}$	$= \frac{-U_2}{\omega_2}$
■	0	+	$= 0$, $= \frac{-\beta_1 U_2}{\omega_1}$	$= \frac{U_2}{\omega_2}$, $= 0$
	0	0	$= 0$	$= 0$
□	0	-	$= \frac{+\beta_1 U_2}{\omega_1}$	$= \frac{-U_2}{\omega_2}$
◇	-	+	$= \frac{-U_1}{\omega_1}$, $= \frac{-\beta_1 U_2}{\omega_1}$	$= \frac{U_2}{\omega_2}$, $= \frac{+\beta_2 U_1}{\omega_2}$
○	-	0	$= 0$	$= 0$
△	-	-	$= \frac{+\beta_1 U_2}{\omega_1}$	$= \frac{-U_2}{\omega_2}$

For example, at such times as u_1 is negative (that is, $u_1 = -U_1$) and $u_2 = 0$, the trajectories must be portions of the two circles shown in Fig. 18.

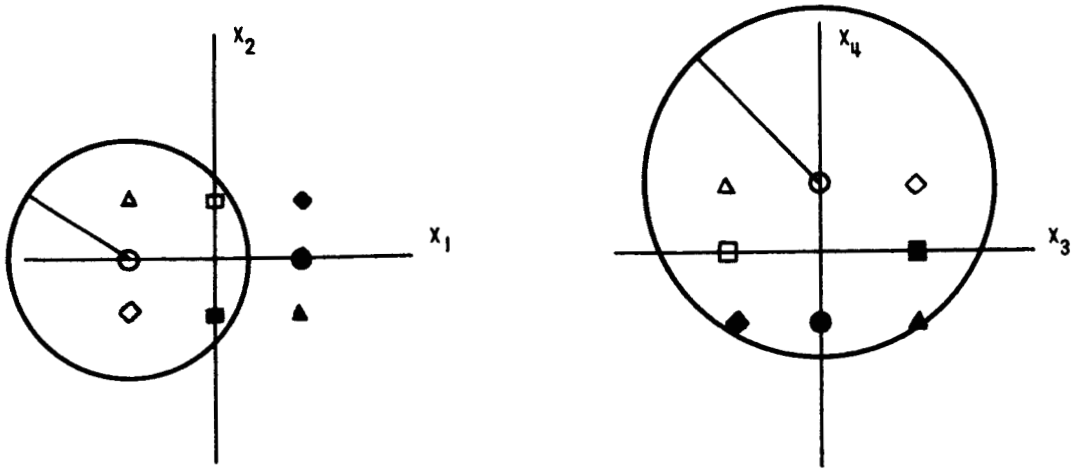

FIG. 18. TRAJECTORY CENTERS.

The problem is when to use what combinations of control action to economize on control effort. The trajectory velocity is of course tangent to the circle and has a value of $r_c \omega_1$ in the nomenclature of Fig. 19a. Maximizing the component E of this velocity directed toward the origin serves to maximize

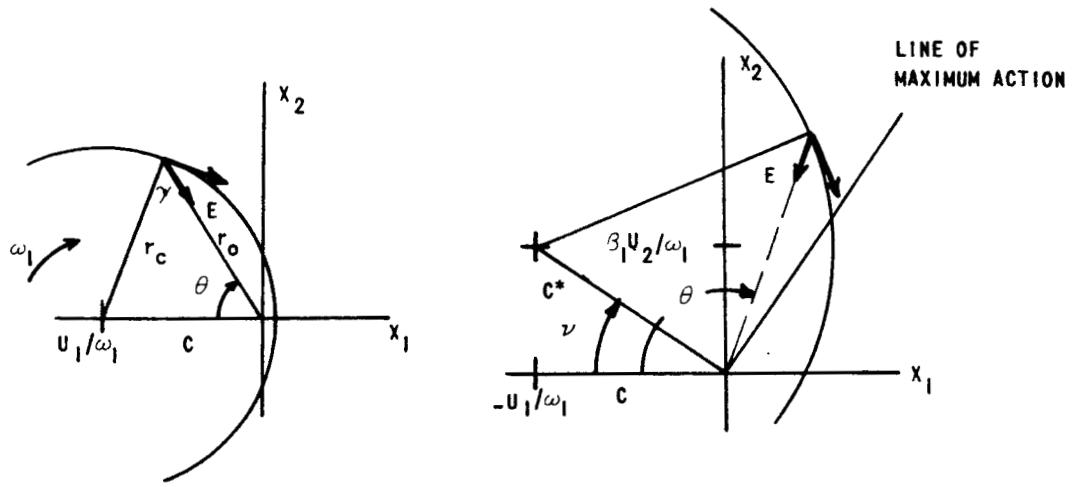

a. One control On

b. Both controls On

FIG. 19. MAXIMUM ACTION LINES.

the benefit of control action because it is desired to zero a disturbance. As in the previous case, this maximum occurs when the trajectory intersects a line normal to the radius vector leading to the center of action; see the following equations. If $r_c > C$,

$$E = r_c\omega_1 \cos(\pi/2 - \gamma) = r_c\omega_1 \sin\gamma = r_c\omega_1 (C/r_c)\sin\theta$$

$$dE/d\theta = 0 = C\omega_1 \cos\theta$$

$$E = \text{max toward origin at } \theta = \pi/2$$

A similar result is true for an off-axis center ($u_1 \neq 0$ and $u_2 \neq 0$) as shown in Fig. 19b, for this case valid if $r_c > C^*$. The maximum action line differs from the above when $r_c < C$ or C^* for the respective cases. Then, θ for maximum E is given by either $\theta = \sin^{-1}(r_c/C)$ or $\theta - \nu = \sin^{-1}(r_c/C^*)$, an orientation which produces $E = r_c\omega_1$. Presuming for the moment that this case with two second-order systems has, for each of the parts, characteristics similar to those found in part A, the best place to expend control fuel is in the region around a line of maximum action. The most efficient application of fuel in an interval between switchings can be found by using the geometry of a sector constructed symmetric about the optimum orientation line. Referring to the case represented in Fig. 20, the duration of control application is equal to $(\eta_1 - \eta_2)/\omega$ and the decrement in distance from the origin, Δr_0, is $(r_{0_1} - r_{0_2})$. A more significant form for the change in r_0 is obtained by normalizing with respect to the control magnitude which caused it. Let $\Delta\hat{r}_0$ equal Δr_0/control magnitude : this has the form of either

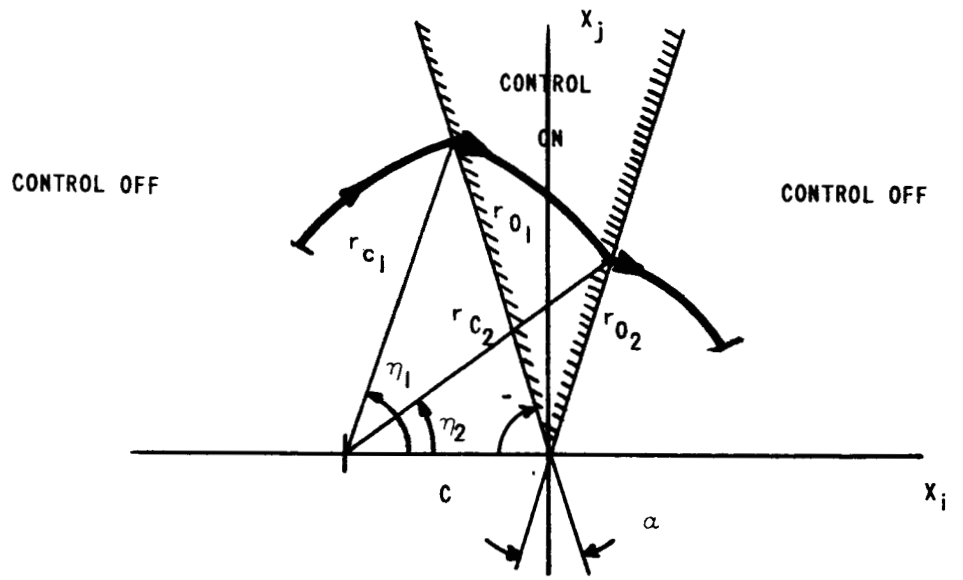

FIG. 20. TRAJECTORY GEOMETRY.

$$\Delta\hat{r}_0 = (r_{0_1} - r_{0_2})/ U_i$$

or

$$\Delta\hat{r}_0 = (r_{0_1} - r_{0_2})/\beta_j U_i$$

The difference $(r_{0_1} - r_{0_2})$ can be found with the help of the law of cosines,

$$r_{c_1}^2 = r_{0_1}^2 + C^2 - 2r_{0_1} C\cos\theta = r_{0_1}^2 + C^2 - 2r_{0_1} C\cos(\pi/2 - \alpha/2)$$

$$r_{c_2}^2 = r_{0_2}^2 + C^2 - 2r_{0_2} C\cos(\theta + \alpha) = r_{0_2}^2 + C^2 - 2r_{0_2} C\cos(\pi/2 + \alpha/2)$$

but $$r_{c_1} = r_{c_2}$$

so $$r_{0_1}^2 - r_{0_2}^2 = 2C(r_{0_1} + r_{0_2})\sin\alpha/2$$

$$r_{0_1} - r_{0_2} = 2C \sin \alpha/2 = \frac{2U_i \sin \alpha/2}{\omega_i} \quad \text{or} \quad \frac{2\beta_j U_i \sin \alpha/2}{\omega_j}$$

For an off-axis case, the C must be replaced with C* as in Fig. 19b. The efficiency of control action is the normalized change in distance from the origin per unit duration of control:

$$\text{efficiency} = k = \frac{(\Delta \hat{r}_0)(\omega_i)}{(\eta_1 - \eta_2)} \tag{51}$$

The efficiency is a maximum of 1 when $\alpha = 0$, indicating that the best method of using fuel is to apply impulsive functions pulsed at each intersection with the maximum action line and to coast in between. For any finite initial $\underline{X}$, this method is going to require quite some time to zero the disturbance, but it might be expected that as T is permitted to increase the control function tends to assume this sort of behavior.

Suppose the control is applied at an orientation other than at the line of maximum action, how is the performance degraded? On selecting a finite sector width $\Delta\eta$ and initial radius from the origin of any value, the ratio of k for a particular orientation, denoted by η_2, to the k for that sector oriented about the maximum action line, $\eta_2 = \eta_{2_0}$, can be found from trigonometric relationships. Such a case is plotted in Fig. 21. An additional effect of rotating the control sector is to change the phase relationships in state space, for $\Delta\eta$ is no longer equal to $\Delta\theta$. This means that trajectories do not encounter a fixed region of control action in state space at intervals of $2\pi/\omega$ in time - a fact which may be of some help in dealing with aperiodic forms of the control law.

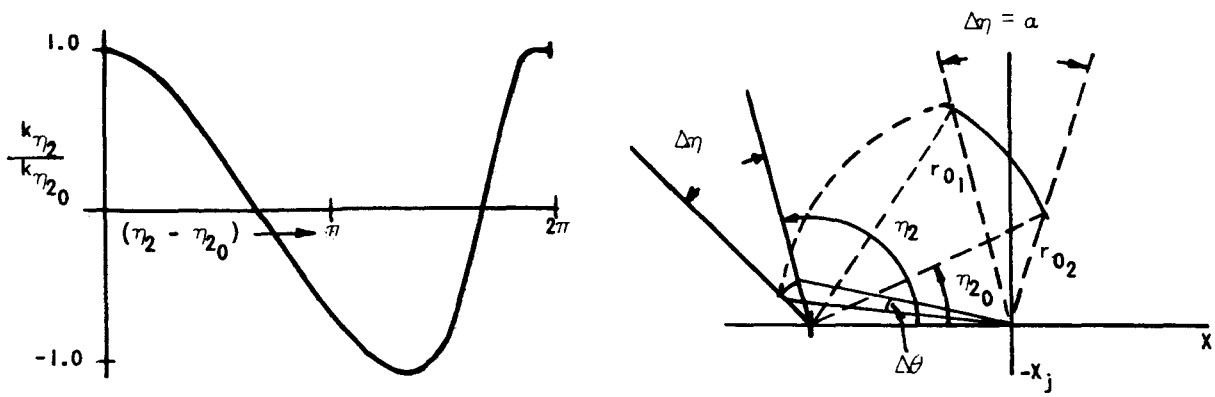

FIG. 21. ROTATED SECTOR RELATIONSHIPS.

Actually one is not so much interested in change of r_0 per unit of control application time as one is in change per unit of fuel. If Q is the rate at which a control expends fuel, k/Q is the criterion which measures fuel economy as a function of choice of control u_1 or u_2, when it is applied, and for how long it is applied. Let k/Q be called the fuel economy index. A consequence is that one would not expect an optimal control to use both controls at the same time unless T is restricted, because the efficiency factor k_{ij} in each plane must now be divided by $(Q_1 + Q_2)$ rather than by Q_1 or Q_2 and the fuel economy index will certainly be less than for one control at a time.

To make use of this knowledge, an estimate of the absolute minimum fuel consumption (the lowest amount of fuel required to zero the disturbance) can be made. Let $R_1(0)$ be the initial un-normalized radius from the origin in the X_1X_2 plane and $R_2(0)$ be that in the X_3X_4 plane. Let the efficiency of the j-th control in the i-th plane be k_{ij}, where subscript "1" will refer to the X_1X_2 plane and subscript "2" to the X_3X_4 plane. These k's can be

un-normalized by multiplying by the appropriate control magnitude (see the definition of k by Eq. (51)). F_1 and F_2 are the total amounts of fuel used by u_1 and u_2 so that

$$\begin{aligned}(U_1/Q_1)k_{11}F_1 + (\beta_1 U_2/Q_2)k_{12}F_2 &= R_1(0) \\ (\beta_2 U_1/Q_1)k_{21}F_1 + (U_2/Q_2)k_{22}F_2 &= R_2(0)\end{aligned} \tag{52a}$$

or, in vector matrix form,

$$M\underline{F} = \underline{R} \tag{52b}$$

Since each of the k_{ij} is held constant for the duration of a solution, the control can be thought of either as one using fixed sectors in state space or one where the average sector orientation produces an average value of k equal to the one used.

The equation can be inverted to yield $\underline{F}$ for a given $\underline{R}$,

$$\underline{F} = M^{-1}\underline{R} \tag{53}$$

It is desired to choose the elements of M so that the sum of the components of $\underline{F}$ is a minimum, which means choosing the values of the k's properly. The best that can be done for k is to make it equal to one. That can be accomplished if the designer is willing to wait long enough, because it requires that every application of fuel occur only when the trajectories in each plane are simultaneously at their respective lines of maximum action. Both $\underline{F}$ and

$\underline{R}$ have only non-negative components, and if a solution to (53) results in positive values of F_1 and F_2 using $k_{ij} = 1$, the answer indicates how to apportion the two controls for least fuel consumption. If one of the F's is negative, it indicates that it is not efficient to use that control for that $\underline{R}$, and that that F should be zero. For example, let the initial condition norm in the X_1X_2 plane be very small compared to that in the X_3X_4 plane; then the control might call for u_1 to be zero, letting $\beta_1 U_2$ decrease the radius vector in the X_1X_2 plane. When this occurs and one of the controls is not used, the two values of k for the other control must be selected in the ratio of the initial conditions so as to insure that the trajectories in both planes arrive at the origin at the same time. That is, suppose $u_1 = 0$, then:

$$F_2 U_2 k_{22}/Q_2 = R_2(0) \quad \text{and} \quad F_2 \beta_1 U_2 k_{12}/Q_2 = R_1(0)$$

so

$$k_{12}/k_{22} = (R_1/\beta_1)/R_2$$

The result is to choose $k_{22} = 1$ and $k_{12} = (R_1/\beta_1)/R_2$. The reduced value of k_{12} is realized by rotating the area of application away from the maximum action line as indicated in Fig. 21. This process will be made more clear when numerical examples are computed in a later section.

Summarizing, a knowledge of the general behavior of the system has been gained from geometric considerations, avoiding for the moment the more difficult mathematical expressions of this case of the Optimal Principle. Of particular benefit is the calculation of a lower bound on fuel consumption as time for solution approaches infinity, which can serve as a basis for comparison for any sub-optimal schemes later proposed. Now the details of the true optimal control can be learned by mechanizing in backward-time the true optimal solutions.

3. True Optimal Solutions

The mechanization described earlier of true optimal solutions in backward time was performed, using these numbers for the problem parameters:

$\alpha_1 = \alpha_2 = 0.5$

$\beta_1 = 0.2 \qquad \omega_1 = .667 \text{ rad/sec} \qquad U_1 = 0.05 \qquad Q_1 = 1$

$\beta_2 = 0.4 \qquad \omega_2 = 1.53 \text{ rad/sec} \qquad U_2 = 0.10 \qquad Q_2 = 2$

The values chosen were arbitrary except to satisfy these criteria:

1) They represent a reasonable satellite configuration.

2) The frequency ratio is non-harmonic so as to represent the most general case.

3) They were compatible with time scaling requirements of the analog computer.

By viewing the two state-space planes X_1X_2 and X_3X_4 simultaneously on two oscilloscopes, the two trajectories were shaped by varying the initial values of the adjoint variables to pass the curves through the respective chosen $X(\tau^* = T)$. After some experimentation, a capability in judging the relative influence of the components of $\underline{p}(0)$ was developed, corresponding to observing or recognizing the shape of the parameter surface being searched and the value of its partial derivatives with respect to the elements of $\underline{p}(0)$.

The series of photographs in Fig. 22 are samples from a set of computer runs for a pair of initial conditions of approximately equal norm value, shown by the scaling diagram to be some three times the size of the primary control power in each plane. The upper half of each photograph is the X_1X_2 plane, the lower half is the X_3X_4 plane, and time for solution is labeled below each pair of plots.

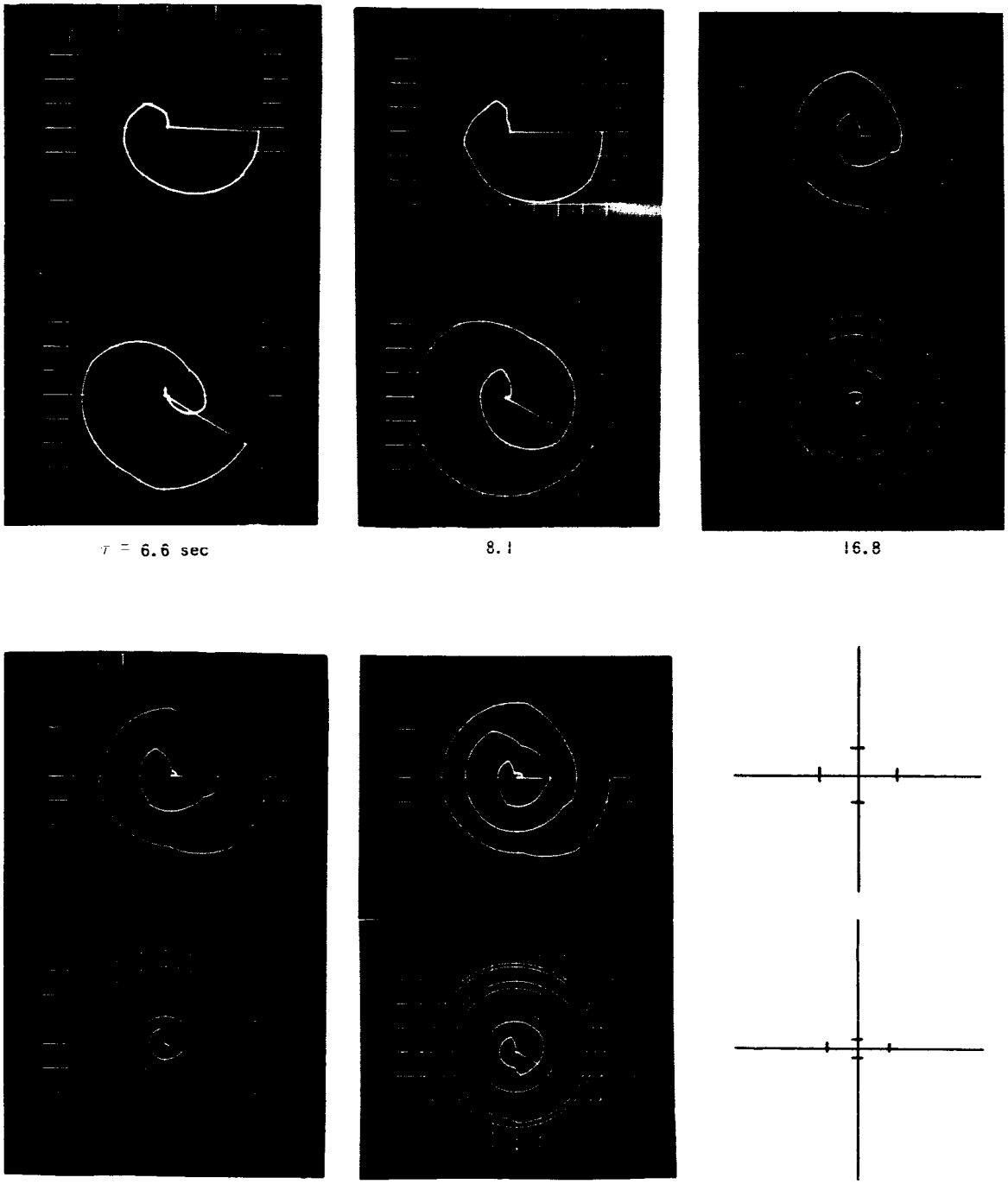

FIG. 22. FAMILY OF TRUE OPTIMAL SOLUTIONS.

Two properties of these solutions are of interest: first, the method in which the true optimal control is applied and its comparison with the ideas suggested by geometric considerations; and secondly, the way in which true optimal solutions trade off increased fuel consumption for decreased time for solution. Taking the latter topic first, a plot of total fuel consumption F, ($F = F_1 + F_2$), versus T for this $\underline{X}(0)$ is given in Fig. 23.

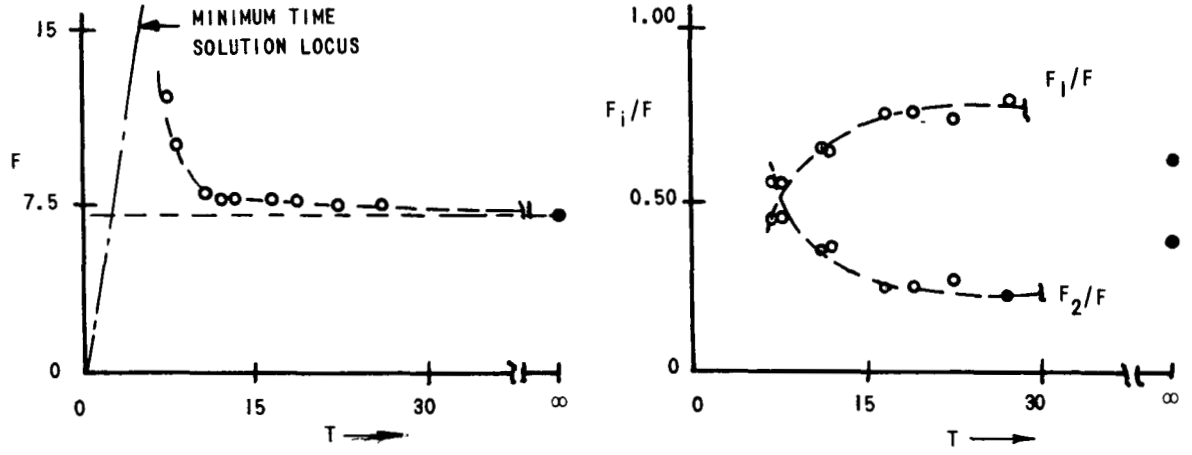

FIG. 23. FUEL USAGE VS TIME FOR SOLUTION.

From these plots it is apparent that F approaches a finite asymptote as T increased in the same manner as with the second-order system, and that the relative use of the two controls is a function of choice of T. If Eq. (53) is solved for this case, the absolute minimum of F is found to be 6.93 units and the relationship of F_1 and F_2 to total fuel is 61.5 and 38.5% respectively (plotted in Fig. 23 at $T = \infty$).*

*The poor agreement between the measured fuel apportionment and the predicted values for infinity was due to mechanization problems on the analog computer, and will be explained later in the text.

The increase in F as T is reduced corresponds to decreasing the average efficiency of each application of control, which makes sense considering that a control could turn on sooner (or more often) if a range of values of k were acceptable, and the only variation possible in k is to lower it. To see if this actually was the case, again return to the first of the two properties of the solutions mentioned on the previous page.

One of the family of solutions shown in Fig. 22 is presented in Fig. 24 much enlarged and accurate enough to measure angles and magnitudes. The two planes have been superimposed, with the respective centers of control marked by crosses for the X_1X_2 plane and by circles for the X_3X_4 plane. One general observation should be made: the choice of this particular solution was based on the fact that for it and all other solutions requiring a larger T both controls were not used simultaneously. This can be seen in Fig. 24 by noting that the centers of trajectory portions were always on one of the coordinate axes. Thus, the behavior previously expected to exist occurred. Other details are best seen by examining each particular control action. Starting at the initial condition, these were the actions of the controls:

1st application - u_1 used - applied slightly early* in X_1X_2 plane, late in X_3X_4 plane.

2nd application - u_2 used - essentially properly timed for $k = 1$.

3rd application - u_1 used - late in the X_1X_2 plane, early in X_3X_4 plane.

4th application - u_1 used - approximately 90^o early in X_1X_2 plane, only slightly late in the X_3X_4 plane.

5th application - u_2 used - 45^o late in X_1X_2 plane, exactly oriented in X_3X_4 plane.

*Early and late refer to timing relative to the same sector width, oriented symmetric about the line of maximum action.

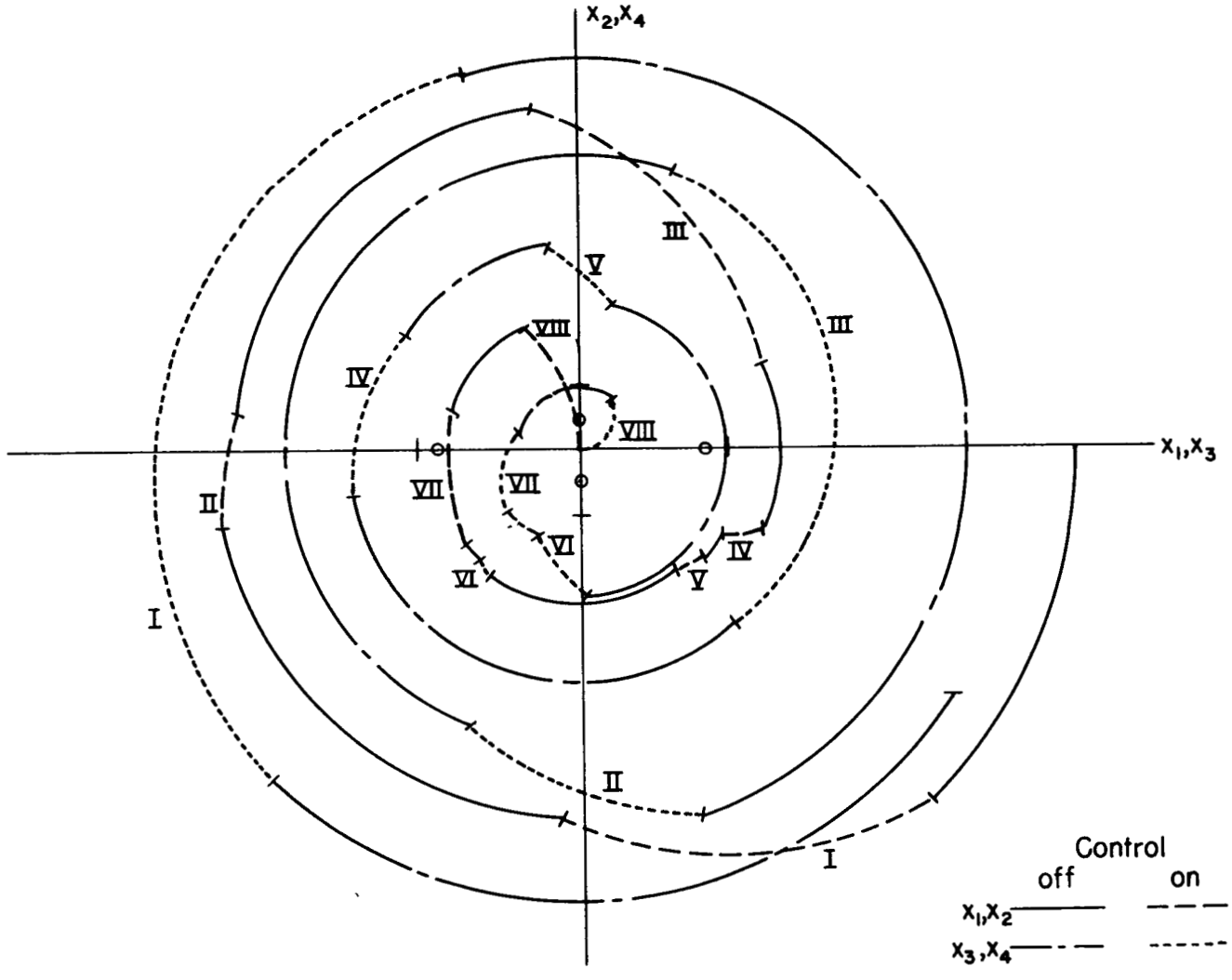

FIG. 24. STATE-SPACE TRAJECTORIES.

6th application - u_2 used - poor utilization in the X_1X_2 plane, slightly late in the X_3X_4 plane

7th application - u_1 used - poor utilization in X_1X_2 plane, k approximately zero; slightly early in X_3X_4 plane.

8th application - u_1 used - optimum application in both planes (a characteristic of all backward time solutions).

Unfortunately, several facts are evident:

1) No two applications of control action had the same duration.

2) The efficiency of application of any particular control was not the same each time it was applied. Thus,

3) fixed areas in state space of control action would not have produced this optimal solution.

Because of the uniqueness of optimal solutions, the series of control actions taken is the only possible series for that value of T. It might be argued that had a different value of T been picked - one from a particular set of values as in the case of the second-order system - the simplicity of control switching sought might have been achieved. Even if this is true, it can be expected that the set of beneficial values of T is much less populated than for that case because now simultaneous simplicity in two planes is required, and this greatly reduces the utility of such a set. Furthermore, providing the ability to calculate and mechanize solutions for these particular values of T does not appear materially simpler than solving the problem directly.

Instead, the family of solutions can be examined to find trends which are common to all values of time and which can be realized by a simple control system. Returning to Fig. 22, some features of the trajectories are encouraging:

1) After sufficient time T was allowed, concurrent use of both controls was not required; the essential format of the trajectory in both planes was established. Further increases in time only slightly modified the

curves and, if anything, tended to make location and duration of control action more nearly constant. The primary difference in solutions thereafter was to decrease the duration of application while increasing the number of times fuel was used. Judging from the F vs. T plot in Fig. 23a, increasing T beyond the point where an effective corner (region of strongest curvature) exists does little in the way of further reducing fuel consumption. Thus, it need only be insured that the mechanization chosen corresponds to some value of T on the nearly horizontal part of the curve to realize a satisfactory compromise in time for solution versus total fuel used.

2) In the faster (X_3X_4) plane, a great deal of the time was spent in coasting while the trajectory was in effect waiting for a favorable orientation in the other plane to occur simultaneously with one in this plane. For example, the control $u_2 = +U_2$, $u_1 = 0$ has a line of maximum action of maximum action at six o'clock in the X_3X_4 plane and at nine o'clock in the X_1X_2 plane, and such a control was used only when both orientations were satisfied (the second application of control in Fig. 24, for instance). An "and" circuit logic could perform the sort of switching in a real system.

3) Of course the true optimal solutions got both trajectories to the origin at the same time (the wisdom of a backward-time synthesis now becomes more evident), but the rate of convergence in each plane was not the same. That is, after one particular control application, R_1 might have been reduced by 10 percent while R_2 was reduced by 7 percent. No discernible pattern was found for any of the solutions. Here the true optimal solution was taking advantage of prior knowledge that whatever happened

at one instance will be supplemented with a reverse or complimentary situation later in the solution to guarantee ending up at $\underline{X} = 0$ simultaneously, and such a capability would be difficult to implement in an actual feedback control. Again it can be said that a different value of T might have produced a situation where the change in R was the same for each application of control, but the same argument as before restricts the utility of using those values of T. A compromise method would be to construct control sectors which do cause a constant change in R, a change in each plane in accordance with the respective magnitudes of $\underline{R}(0)$.

4) The relative apportionment of F_1 and F_2 varied with T as shown in Fig. 23b. To emulate this would require some measure of complexity in a mechanization, so as an alternative, impose that mixture of the two controls which is thought to provide the absolute minimum fuel consumption - the mixture dictated by Eq. (53) with $k_{ij} = 1$ - and fix the control at that amount.

To check the general applicability of these hypotheses and observations, four additional families of solutions were obtained using four widely different sets of initial conditions. Detailed plots like those in Figs. 22 and 23 are given in Appendix F, but the significant trends are given in the table below. The use of the philosophy which resulted in Eq. (53) seems justified in view of the agreement of these measured data with the predicted values. Lack of close agreement can be attributed to the comparison of the value of T at which the data were taken with infinity.* More pertinently, it is not that the magnitude

*Due to mechanization problems with the analog equipment, solutions for values of T larger than those in the table did not produce dependable results.

TABLE II. COMPARISON OF RESULTS

			Measured Performance (Optimum, Backward Time)				Performance Computed From Eq. (53)			
Family	$R_1(0)$	$R_2(0)$	F	T	F_1/F	F_2/F	F	T	F_1/F	F_2/F
A(Fig. 22)	0.24	0.219	7.95	27.9	0.79	0.21	6.94	∞	0.615	0.385
B	0.18	0.027	3.69	19.2	1.0	0.0	3.60	∞	1.0	0.0
C	0.06	0.30	7.02	21.3	0.29	0.71	6.00	∞	0.0	1.0
D	0.30	0.144	6.90	30.0	1.0	0.0	6.00	∞	1.0	0.0
E	0.18	0.12	5.85	28.5	0.81	0.19	4.44	∞	0.76	0.24

of T should be compared to infinity but that the magnitude of T should be compared to T at the effective corner in the F-T curve. That is, the solutions will approach the soultion for $T = \infty$ when T is large compared to T at the corner.

From these considerations it is now possible to formulate a realizable control.

4. Mechanization of a Control

The central concept of the control scheme is to be that a control shall be created whose elements are fixed in the pattern of the true optimal solutions requiring infinite time, but use finite durations of control application rather than impulsive applications. Hopefully, the resulting compromise will provide only a small increase in fuel consumption over the true optimal control. The following features of the control are essential:

1) Fixed sectors of control application will be used.

2) Orientation of the sectors will be as per Eq. (53).

3) The ratio of the two controls will be in accordance with Eq. (53) with $k_{ij} = 1$ assumed.

4) T will be limited to those values greater than T at the effective corner in the F-T curve, thus guaranteeing use of only one control at a time.

Before commencing the actual mechanization, the topic of a primary unit of control must be explained. Equation (53) dictates a ratio of fuel apportionment between the two controls and the total amount of fuel to be expended, but does not directly include the effect of duration of each application of control. If the limiting case of $T \rightarrow \infty$ is being computed, each application is assumed to be impulsive. The ratio F_1/F_2 then represents the ratio of number of impulses used by each control. (Actually, since the magnitude of each pulse is fixed by the bound on that control an infinite number of pulses of each control is used as pulse duration approaches zero. The ratio is construed to mean the limit of the ratio of number of pulses as pulse width approaches zero.) When finite pulse duration is used, it is desired that the probability of encountering a section for control u_1 be a multiple of the probability of encountering a u_2 sector. The factor indicating this multiple shall be in accord with the ratio of fuel apportionment given by Eq. (53). The simplest way of doing this is to ratio the sector widths. If the control which is required to be on the longer portion of T is selected as the primary control, its sector width α^* can be chosen to provide some measure of control of time for solution (as choice of N was used in Eq. (20)). The secondary control sector width α_s is then made to be less than α^* by the desired ratio. Because time of application is the same in both planes, either plane may be chosen as the basis for mechanization, scaling the sector widths in the other plane with due respect to the ratio of frequencies.

To select α^*, a method analogous to choosing N for the second-order case is desired. Such a method, one which sets upper and lower bounds on the value of T for a given sector width, is available as a by-product of the

computation of the secondary sector width. When both controls are to be used, it is desired to make the probability of encountering a situation where the secondary control (the one requiring less duration of control effort) is used to be some fraction of the probability of using the primary control. For example, suppose that F_1 is found to be greater than F_2 or more pertinently that F_1/Q_1, the total duration of control action by u_1, is found to be greater than F_2/Q_2. Then the control should occur in the ratio $(F_2/Q_2)/(F_1/Q_1)$, or, that should be the ratio of probability of using u_2 to the probability of using u_1. The probability of using one polarity of any control, say $u_1 = + U_1$, (which will hereafter be written as $p_{u_1=+}$, for the sake of simplified notation) is the joint probability of the trajectory projected into each plane being in a favorable orientation. If the phase angles in each plane are statistically independent, this is the product of the individual probabilities of occurring in the separate planes.* In either plane, the probability is simply the sector width divided by 2π. Thus, the joint probability of $u_1 = +$ is

$$p_{u_1=+} = \left(p_{u_1=+} \right)_{12} \cdot \left(p_{u_1=+} \right)_{34} \tag{54}$$

$$= (\alpha^*/2\pi)(\omega_2/\omega_1)(\alpha^*/2\pi) = (\omega_2/\omega_1)(\alpha^*/2\pi)^2$$

and similarly the joint probability of $u_2 = +$ is

$$p_{u_2=+} = (\omega_2/\omega_1)(\alpha_s/2\pi)^2 \ . \tag{55}$$

Consequently,

$$p_{u_2}/p_{u_1} = (\alpha_s/\alpha^*)^2 \ . \tag{56}$$

*As will be shown in a later example, statistical independence of phase angles will be sufficient grounds for requiring that the frequency ratio in the two planes be a non-integer relationship.

To satisfy simultaneous arrival at the origin of the trajectories, Eq. (56) must be made equal to the ratio of control duration, i.e.,

$$p_{u_2}/p_{u_1} = (F_2/Q_2)(F_1/Q_1) \quad . \tag{57}$$

Finally, then, it is always true that if both controls are to be used (see Eq. (56)),

$$\alpha_s = (F_i Q_j / F_j Q_i)^{1/2} \; \alpha^* \tag{58}$$

where

$$F_i/Q_i < F_j/Q_j$$

To find the bounds on T that go along with these sizes of α^* and α_s, the amount of time required to expend the amount F_1 of fuel, if the probability of using u_1 is p_{u_1}, must be

$$T = (F_1/Q_1)/p_{u_1=+} \tag{59}$$

This then provides an upper and lower bound on T, for if the initial phase angles in state space were such to require the use of only one polarity of u_1, the entire amount of F_1 constitutes the numerator of the right-hand side of Eq. (59); whereas, the shortest time required to expend fuel is when exactly half the value of F_1 is used by positive control action and the other half by negative action. So,

$$(F_1/Q_1)/2p_{u_1=+} \leq T \leq (F_1/Q_1)/p_{u_1=+} \tag{60}$$

Since α_s was determined with the same statistics, an identical answer results if the calculations are based on u_2 and F_2.

A range of T exists because only the magnitude of the norm of the initial conditions has been considered, ignoring for the moment the phase angles in state space. If the size of the norms are kept constant and the phase angles varied it could be expected to encounter one pair of phase angles which required the upper bound on T and a different pair which required the lower bound. Since the designer will have a better knowledge of the statistics of the size of the initial conditions than he would of the relative sizes among the components of the initial condition vector, the bounds are of significance.

Another problem must be dealt with before proceeding. Requiring that the projection of a phase point in one plane be in a satisfactory region at the same time that the projection of the phase point in the other plane is also in a favorable region presents some difficulty. For it is one thing to provide an and-logic for detecting when two projections of the phase point are simultaneously within their respective sectors, and another thing to detect when both projected phase points simultaneously enter their sectors. In the sketch below, the consequence of requiring only that both projections of the phase point be within sectors is seen to be that the effective duration of the application is reduced and that the orientation of the effective action is rotated in each plane. Fortunately, the state space phase shift accompanying the cocking of the sectors is such to try to reorient them toward the desired line of maximum action.* This situation will be tolerated in the mechanization for these reasons: first,

*A short proof is given in Appendix G.

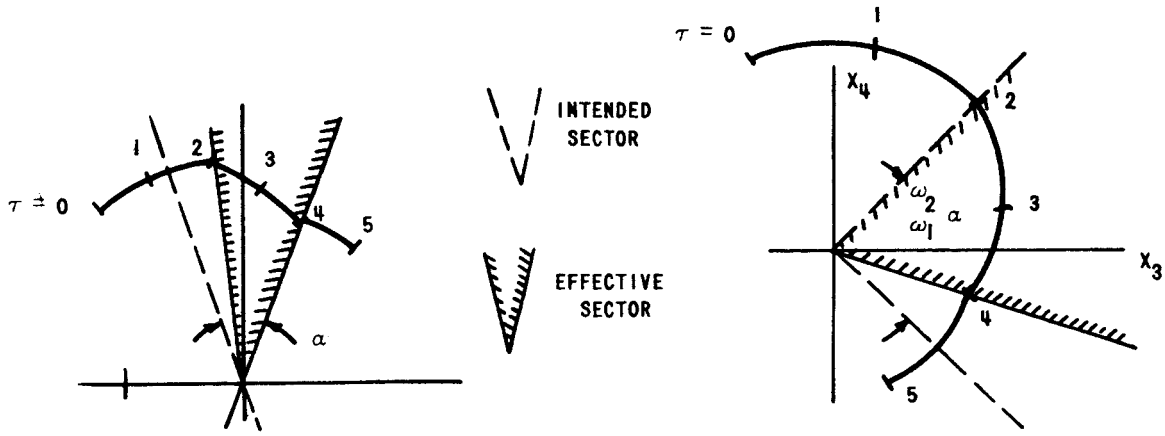

FIG. 25. COINCIDENT SECTOR RELATIONSHIPS.

it occurred in the true optimal backward time solutions. The slight decrease in efficiency k is not significant and the phase shifts appeared to shorten the time required to obtain coincidence of favorable applications; that is, essentially the same fuel is used for a shorter T.** Secondly, computing coincidence of entering a boundary line of control application is an added complexity which does not appear worth the cost, particularly since T is not appreciably increased by the simpler method.

The actual mechanization can now be considered. Figure 26 presents a block diagram of the actual control and the best way to understand its workings is to use a sample set of initial conditions to solve for each of the elements of the control.

Inputs to the control computer consist of initial conditions $\underline{X}(0)$, either a preselected value of α^* or the upper bound on T as a basis of computing

** If the slope of F(T) after the effective corner is considered practically to be zero.

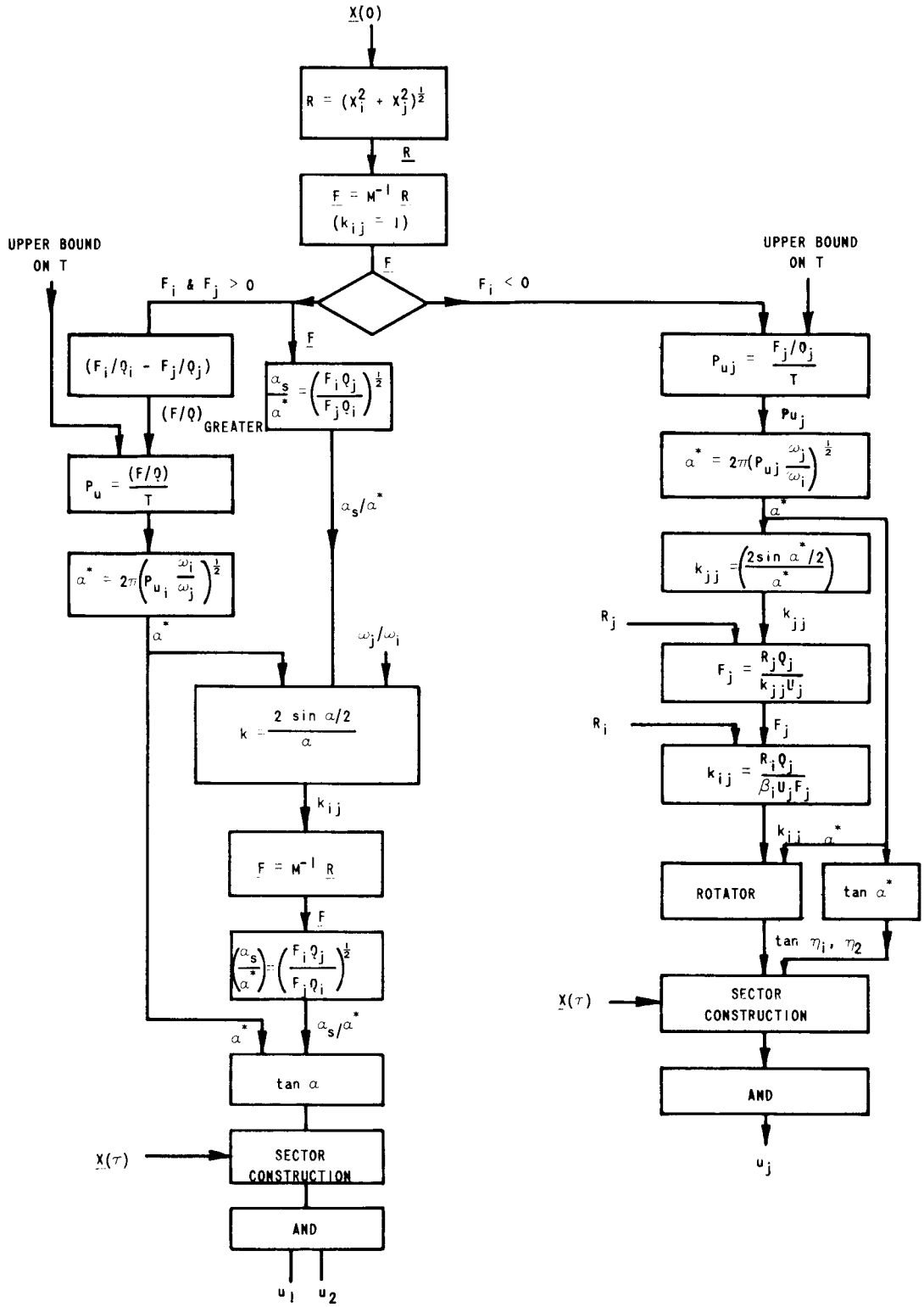

FIG. 26. CONTROL COMPUTER BLOCK DIAGRAM.

α^*, and the state vector as a function of time $\underline{X}(\tau)$ for generation of sectors. If the value of α^* is to be preselected and held constant for a given plant, it should be based upon satisfying the largest expected initial condition within the allotted time. For completeness, computation of α^* is included as a capability of the control computer in Fig. 26. The test case will be one which represents a maximum expected $\underline{X}(0)$ for a gravity-gradient stabilized vehicle like the Agena.* The runs labeled A in Table II (p. 64) are of the proper size.

Calculation of the norms in each plane is the first step. For the data of run A, these are found to be 0.24 and 0.219 in the X_1X_2 and X_3X_4 planes respectively. Using the computed norms, the performance of the control for an infinite time for solution is gotten by solving Eq. (53) with $k_{ij} = 1$.

F_1 and F_2 are then inspected to determine positive definiteness. If both values for fuel are greater than zero, both controls are to be used and the left-hand path of logic is followed. For the test data this is the case, F_1 being (0.615)(6.94) and F_2 being (0.385)(6.94). (See Table II, page 64). The right-hand logic path is selected if either F_1 or F_2 is less than zero and will be explained later.

Taking the desired upper limit on T to be 150 seconds (in scaled time, τ,), in the next block the desired probability of encountering the primary control is computed. Since F_1/Q_1 is greater than F_2/Q_2 for the test case, ($Q = 1$, $Q_2 = 2$) u_1 is the primary control and $p_{u_1=+}$ is computed:

$$p_{u_1=+} = F_1/Q_1T_{max} = (0.615)(6.94)/(1)(150) = 0.0284$$

*Scaling of the initial conditions is given in Appendix H.

The primary sector width α^* can then be found by use of Eq. (54):

$$\alpha^* = 360^o \quad (p_{u_1=+})/(\omega_2/\omega_1)^{1/2}$$

$$= (360)(0.0284/2.28)^{1/2} = 40^o .$$

This value now forms the primary control unit for the system.

In parallel with this computation, secondary sector width is computed in terms of α^* by means of Eq. (58):

$$\alpha_s/\alpha^* = (F_2Q_1/F_1Q_2)^{1/2} = (0.385)/(0.615)(2)^{1/2}$$

$$= 0.56$$

This result, plus the computed value of α^* (40^o), permits calculation of the values of k_{ij} to be used for a finite control.

Values for k_{ij} are computed using Eq. (51) in the form

$$k = \frac{2 \sin (\alpha/2)}{\alpha}$$

and recalling that values of α^* and α_s in the X_3X_4 plane are in the ratio of $\omega_2/\omega_1 = 2.28$ to those in the X_1X_2 plane. The efficiencies are:

$$k_{11} = \frac{2 \sin (40^o/2)}{(40/57.2)} = 0.975$$

$$k_{21} = \frac{2 \sin \left[(2.28)(40^{\circ}/2)\right]}{(2.28)(40)/(57.2)} = 0.88$$

$$k_{12} = \frac{2 \sin \left[(0.56)(40^{\circ}/2)\right]}{(0.56)(40)/(57.2)} = 0.97$$

$$k_{22} = \frac{2 \sin \left[(0.56)(2.28)(40^{\circ}/2)\right]}{(0.56)(2.28)(40)/(57.2)} = 0.97$$

With these new k's, Eq. (53) is again solved, this time representing fuel usage for finite sector widths. The results are $F_1 = 4.31$ and $F_2 = 2.97$, an increase in total fuel consumption of 0.34 units over the infinite time fuel consumption. Apportionment of fuel is changed by less than 2%. Because of the increase in primary fuel consumption, the estimate on time is slightly low, that is, the upper bound on T has increased by the increase in F_1 if α^* is kept at 40°. The error is small: the bounds on T are now $76.5 \leq T \leq 153$.

In the following blocks, the ratio α_s/α^* is recomputed and the tangents of α_s, α^* in both planes are determined. These are used with the state variables to determine sector construction. Finally an and-logic detects mutual occupancy in control sectors in both planes and switches u_1 and u_2.

For the alternate logic path, if one of the values of F is less than zero when computed for an infinite time solution, the other control is to be used and the first block in this path calculates the probability of using that control to satisfy the upper bound on T. As with the previous description, α^* is computed and an efficiency and F are found for a finite sector width. Efficiency in the secondary plane is determined in the manner of the example on page 55. To effect that value of k, the block labeled "rotator" serves to orient the control sector away from the maximum action line by an amount necessary to produce an average efficiency equal to the desired k. As with the other case, the

final step is to construct switching lines in state space and and-logic for switching the control to be used.

All of the elements of logic can be and were accomplished with simple analog computing components, the most difficult task being rotation of sector orientation. Here the only compromise in the control scheme was made, as indicated by the words "average efficiency" in the previous paragraph. The borders of sectors which produce constant efficiency are not straight lines in state space because the orientation varies with size of the norm, but the approximation is not penalizing and is justified by the attendant simplicity. By taking the straight line approximation, a diode function generator provides an output of the tangents of switching line angles for an input of desired k.

5. Estimating Minimum Time Performance

If an estimate of the fuel and time required for a least time solution were available, the designer would have a basis for comparison of the economy of his mechanized least fuel solution. These estimates can be obtained by further exploiting the concepts which led to Eq. (53). The task is to try to find a set of values of efficiency, k, to use in the matrix M^{-1} of Eq. (53) that tend to represent the shortest possible time for solution. The essential difference between that situation and the least fuel case is that the control is on all the time in minimum time problems. If the control is on continuously, fuel is proportional to time:

$$F = (Q_1 + Q_2)T \tag{61}$$

Thus, efficient expenditure of fuel is efficient expenditure of time and the least time control must therefore be efficient in fuel usage for that time T. In addition, the minimum time solution belongs to the family of minimum fuel solutions and constitutes the left-hand end point in the fuel versus time curve; it can be thought of as a limiting case of the least fuel problem where the ratio of the maximum amplitudes of the adjoint variables to U_i approach infinity, reducing the coast time to zero and simply making u approach the sgn(f).

The most efficient manner to apply a least time control is to: (1) limit the maximum duration of control action by one polarity to one-half a period; and, (2) orient these sectors of control action symmetrically about the maximum action line. The reason for the first condition is that any application of fuel for a time greater than half its period must have some portion where the trajectory is being driven away from the origin; the reason for the second condition has been explained before. Consequently, it shall be postulated that the least time control has, as the average condition in its best case, primary sector widths of 180^{o} for each of the primary controls in their respective planes. The other sectors are then the projections into the alternate plane, scaled by the frequency ratio. The k's can now be computed:

$$k_{11} = k_{22} = \frac{2\sin(\pi/2)}{\pi}$$

$$k_{12} = \frac{2\sin\left[\pi/2(\omega_2/\omega_1)\right]}{\pi/(\omega_2/\omega_1)} \qquad (62)$$

$$k_{21} = \frac{2\sin\left[(\omega_2/\omega_1)(\pi/2)\right]}{\pi(\omega_2/\omega_1)}$$

(This corresponds to an apportionment factor ω_1/ω_2.)

Knowing M^{-1} now and substituting for F in terms of T by means of Eq. (61), Eq. (53) can be used to obtain two equations in T. If both values of T agree it means a set of initial conditions have been found incidentally where the estimation techniques are exact. For the general case where the values of T are not the same the scheme could be corrected by seeking the largest values of k_{ij} which produce equal values of T in both equations - that is, perturbing slightly about the values of k_{ij} found in Eq. (62). Since the values of k_{ij} can only be diminished from those found in Eq. (62), the resulting T would be larger. Only a lower bound is sought so that use of these values in comparing fuel savings in the least fuel scheme is conservative anyway and the perturbation technique need not be used.

For the initial conditions of run A in Table II, (page 64) use of this technique results in $F = 3T$ from Eq. (61) and the values of k from Eq. (62) are $k_{11} = k_{22} = 0.638$, $k_{12} = 0.92$, and $k_{21} = 0.062$. Substituting these into Eq. (53) yields a T of 4.77 seconds (the larger of the two values of T). Consequently based on this estimate it would require 14.31 units of fuel to do the job in least time.

6. Performance of the Sub-Optimal Control

Performance of the actual control is given in the table below. Run A-1 had initial conditions identical with the original runs for A - those pictured in Fig. 22 - while A-2 and A-3 are samples from several runs which had the same norms but different initial phase angles in state space. (Phase angles in X_1X_2, X_3X_4 were 0, -34^o for A-1; 180, -34^o for A-2; and 90, -75^o for A-3.)

TABLE III. PERFORMANCE COMPARISON

$R(0) = (0.24, 0.219)$

$\alpha^* = 40^o$

	F	T	F_1/F	F_2/F	R(T)
Actual Control Runs:					
Run					
A-1	7.28	93.0	.65	.35	(0.0015, 0.0135)
A-2	7.65	82.5	.59	.41	(0.00 , 0.006)
A-3	6.83	90.9	.605	.395	(0.00 , 0.024)
True Optimal (Backward Time) Solution:					
A-1	7.95	27.9	.79	.21	(0.0 , 0.0)
Estimated Performance (from Eq. 53):					
	6.93	∞	.615	.385	(0.0 , 0.0)
	7.28	(76.5-153)	.62	.38	(0.0 , 0.0)
Estimated Minimum Time Solution (from Eq. 53):					
	14.31	4.77	.666	.333	(0.0 , 0.0)

Representative selections from a group of runs are given, and the agreement is felt to be quite good concerning fuel consumption with slight variations in performance seen to be caused by varying initial phase angles. The value of total fuel consumption for run A-3 appears to be less than that for an infinite time solution only because the problem was stopped before both trajectories were completely zeroed, as indicated by a final value of R, R(T), of 0.0 and

0.024. Typically, when one of the trajectories reaches the origin before the other, the small signal level causes noise and indecisive switching action in the relays and in the "and" circuits. In practice a dead zone could be constructed around the origin in each plane to remedy this effect, shunting one of the elements to the "and" logic if that trajectory was already within its dead zone, and opening both control logic elements if both trajectories were within their dead zones.

To obtain a time for solution more compatible to those observed in the true optimal backward time solution, α^* was increased to 60°. The predicted performance, from Eq. (53), was a total fuel consumption of 7.72 units and bounds on T of 34.05 and 68.1 seconds. Actual runs by the mechanized control gave results of 7.8 units for fuel consumption and a time of 36 seconds for the initial conditions of A-1. The effectiveness of increasing α^* is perhaps better seen in comparing Figs. 27 and 28 where time histories of the components of the state vector was given.

Turning to a situation where only one control is required, the estimation techniques described applied to the initial conditions of run B produce an F of 3.69 with $64 \leq T \leq 128$ seconds for an $\alpha^* = 40^\circ$. Computer runs showed an average F of 3.83, T = 103.5 seconds, and R(T) = (0.0045, 0.003) for a variety of initial conditions but a constant norm, R(0), of (0.18, 0.027). A time history plot is shown in Fig. 29.

7. Difficulties of the Scheme

Two difficulties arise in using the method of control, and they may be illustrated by a single example. If the case is taken where the frequency

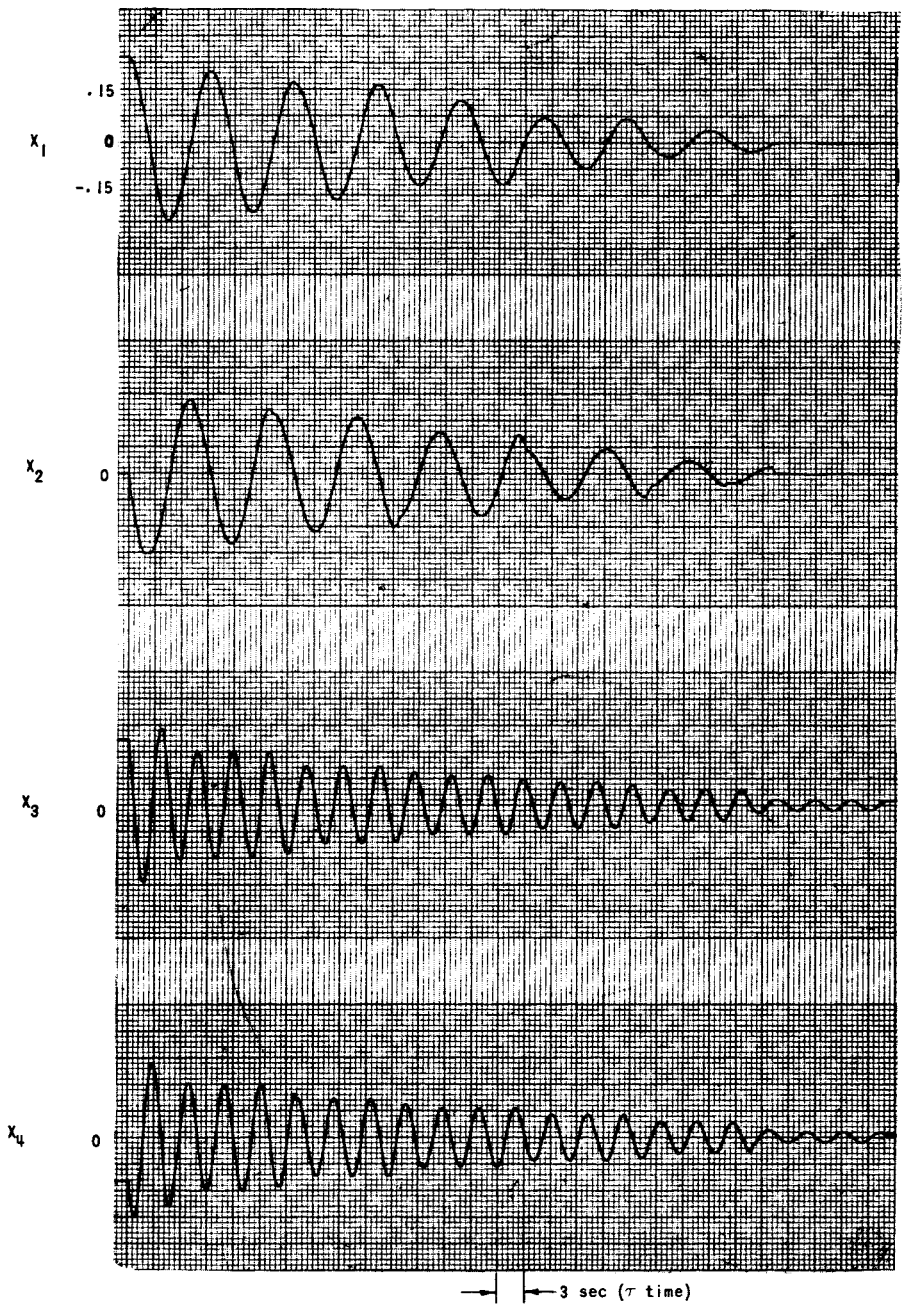

FIG. 27. TIME HISTORY, INITIAL CONDITION A, ($\alpha^* = 40^\circ$).

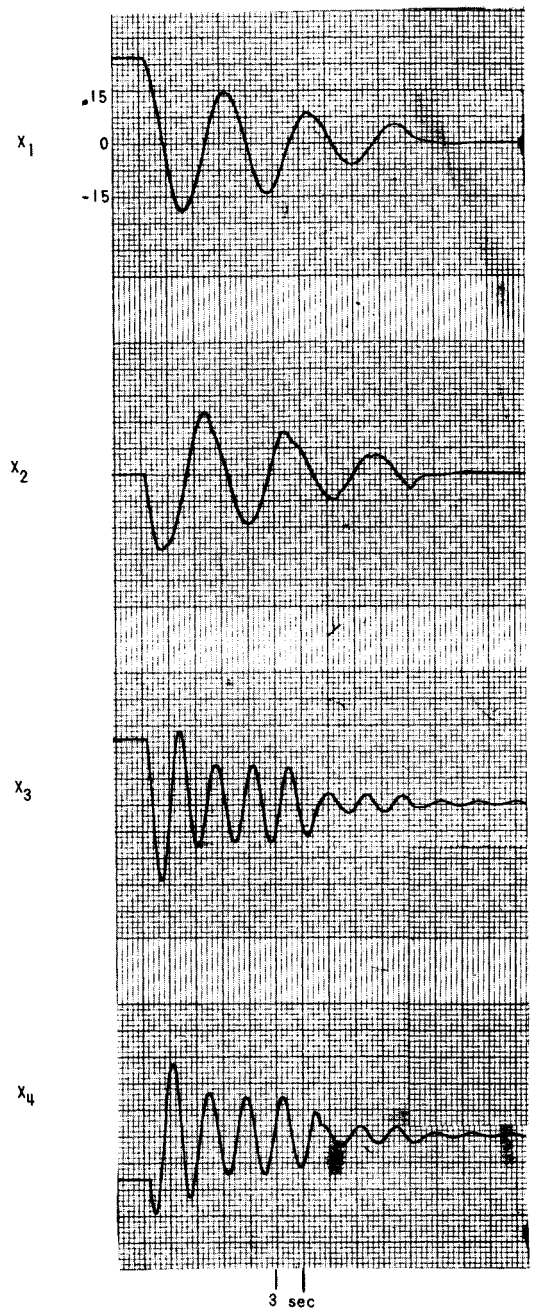

FIG. 28. TIME HISTORY, INITIAL CONDITION A, ($\alpha^* = 60^\circ$).

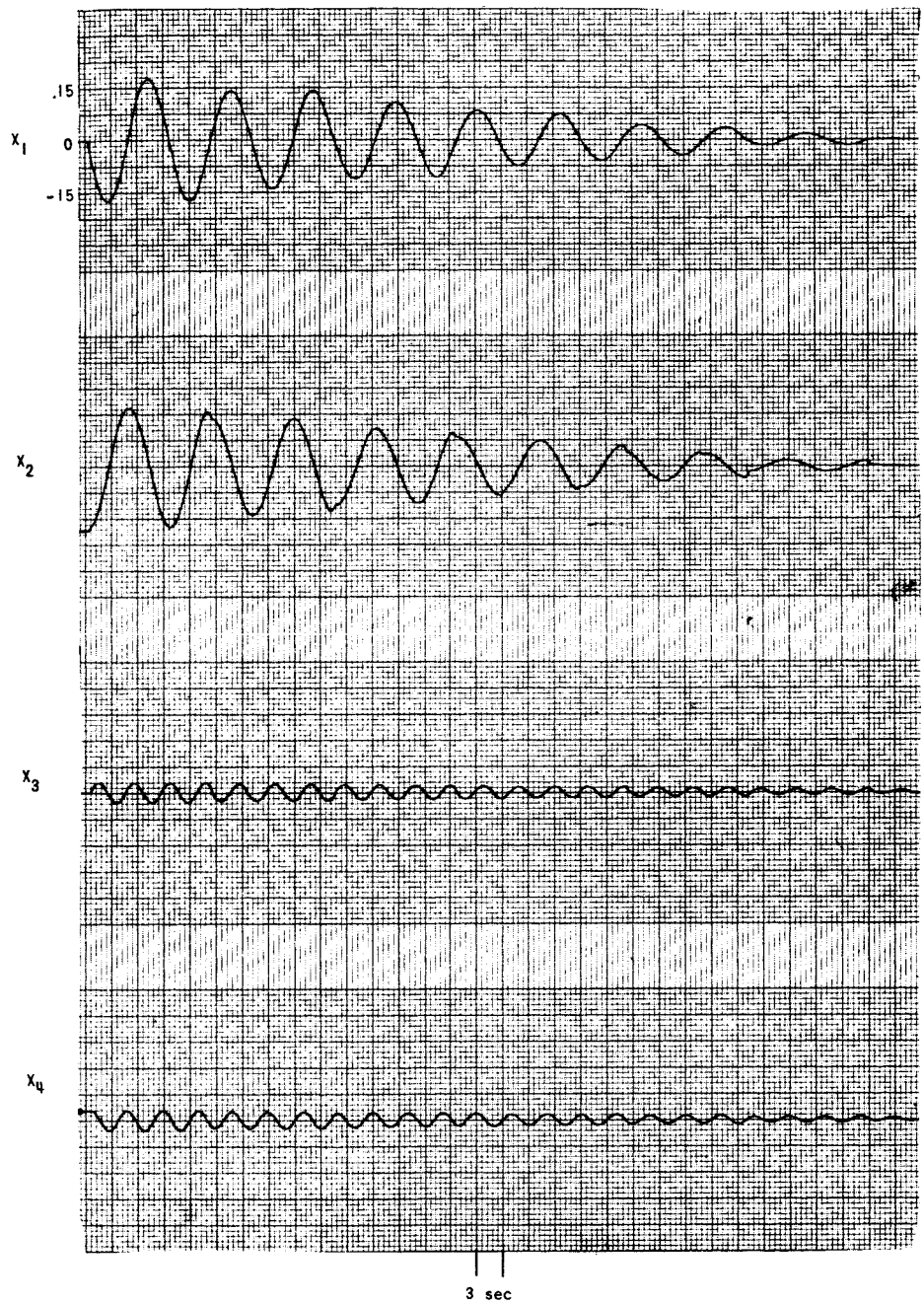

FIG. 29. TIME HISTORY, INITIAL CONDITION B.

ratio between the two planes is large and where the ratio is an integer - say 8.0 - both problems manifest themselves. The first complication is a limitation on the size of the primary sector width. If α^* is chosen for the slower plane, its projection in the other plane may exceed 360^o, a situation producing confusion or complexity in the switching logic. And if α^* is limited to be less than $(360)/(\omega_2/\omega_1)$, the time for solution may be much longer than is desired. A possible solution would be to detect coincident entrance into mutually favorable locations and simply provide a time interval of control equivalent to the sector angle greater than 2π. This has all the attendant difficulties spoken of before.

The second difficulty is more easily overcome. The source of trouble is the integer ratio of the frequencies. Taking a satellite whose geometry results in a large frequency ratio, a near limiting case for a gravity-gradient stabilized configuration occurs for $\omega_1 = 0.15$ and $\omega_2 = 1.2$. Strong coupling accompanies this arrangement, β_1 being 0.25 and $\beta_2 = 0.73$. In actual runs with the mechanized control, time histories showed that typically the trajectory in one plane reached the origin far sooner than did the trajectory in the other plane. Figure 30 presents such a plot. Which of the trajectories was nulled first depended strongly upon the initial phase angles in state space, a condition caused by the fact that with harmonic frequency relationships the phase relationships are preserved throughout a time of solution. That is, the state space patterns tend to be repetitive in time and thus suffer poor mixing of phase angles. As a consequence, the joint probability required for a control to be on is no longer the product of the probabilities in each plane: the two planes are now no longer statistically independent. Figure 31 shows the considerable improvement obtained when we alter the frequency ratio only slightly

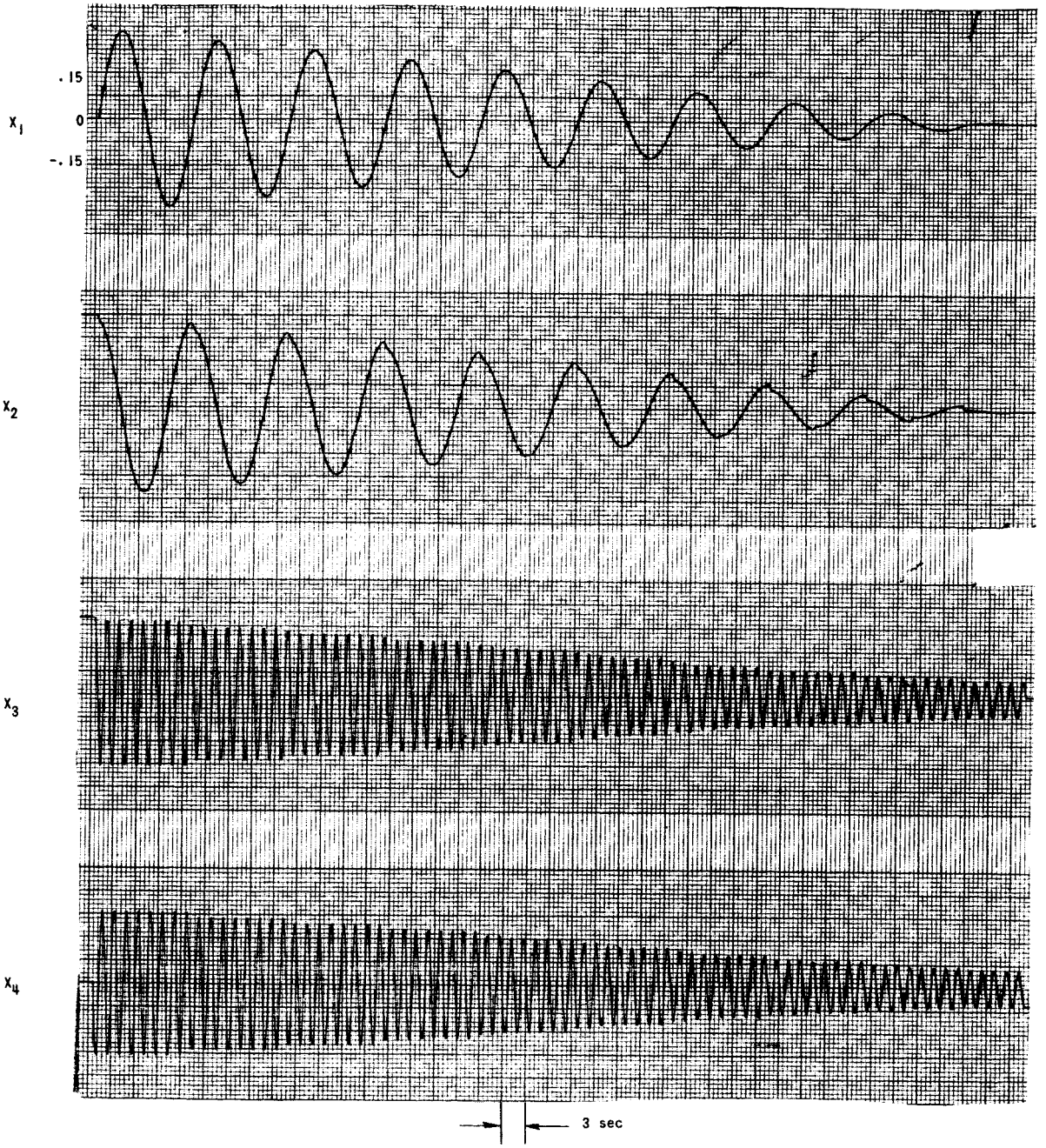

FIG. 30. TIME HISTORY, $\omega_2/\omega_1 = 8.0$.

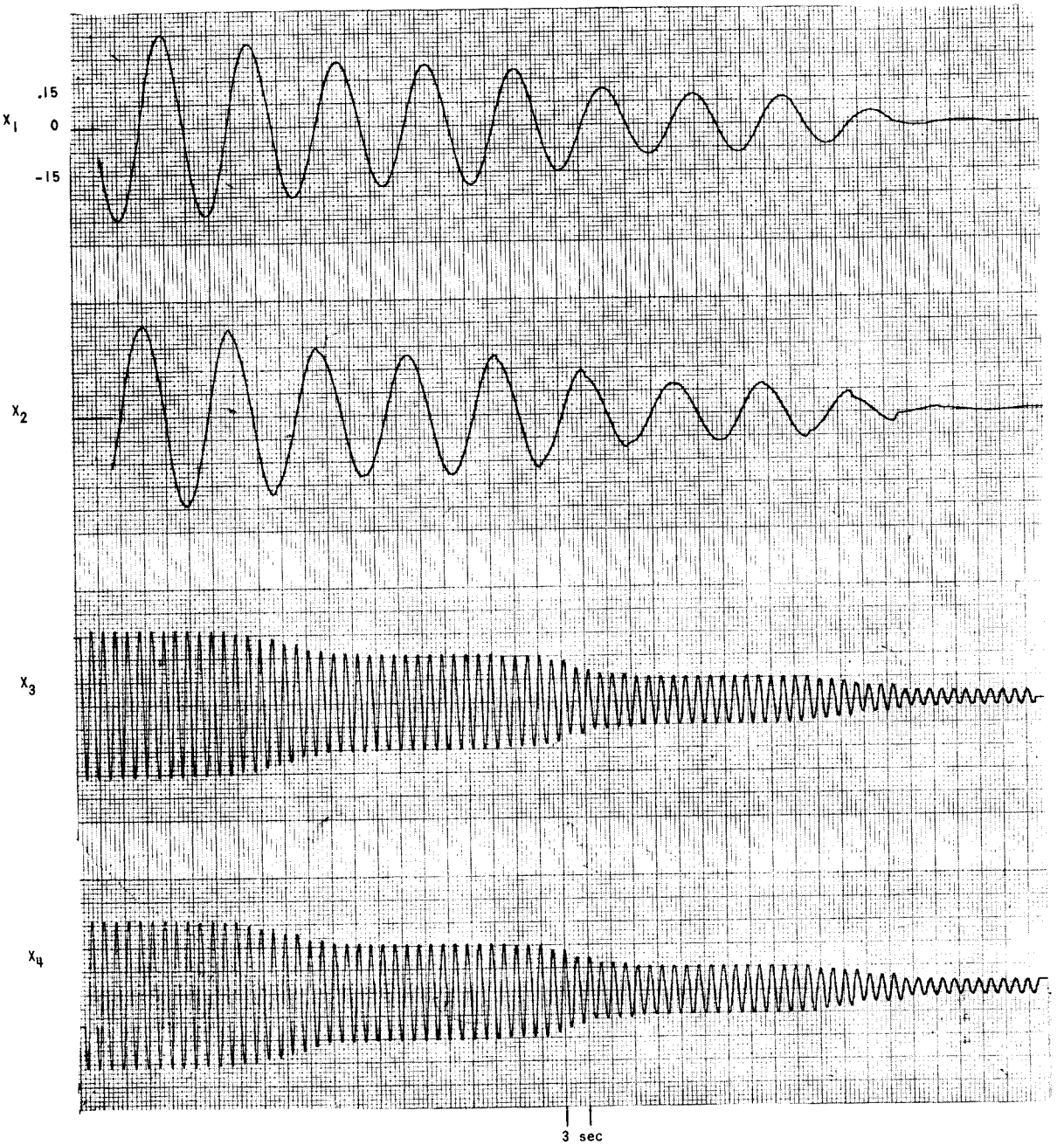

FIG. 31. TIME HISTORY, $\omega_2/\omega_1 = 7.63$.

to 7.63. Now a definite "beat-frequency" effect is apparent from the amplitude envelope of the time histories and the trajectories now close to the origin synchronously. The stipulation is then that the designer should choose moments of inertia of the satellite to insure a non-integer ratio of the natural frequencies - surely not a prohibitive restriction.

Finally, one additional thing, although not actually a difficulty, should be commented upon. Should the initial condition in one plane be identically zero, how is the control accomplished? While it does not intuitively seem efficient to do so, true optimal backward time solutions showed that the trajectory originally at the origin was driven out and then back in again in the course of dealing with the trajectory in the other plane. A sample of such a case is given in Fig. 32 for a frequency ratio of 2.28, the same as for runs A through E, with an initial norm of $R(0) = (0.18, 0.0)$. Here the X_1X_2 and X_3X_4 planes are superimposed, the outer or larger trajectory being that in the X_1X_2 plane. In essence what happens is that as per Eq. (53), only the u_1 control is used and its projection in the X_3X_4 plane is oriented such that the average k is zero. For the actual control, the method of employing dead zones could be used to circumvent the "and" logic until the trajectory that was originally zero had been driven outside the dead zone. At that point, the states could be "sampled" to give the control computer a new set of initial conditions to reformulate the control. In fact, as mentioned in the second-order control section, it is generally desirable to cause the states to be sampled at some interval and to have the control recomputed each time, because that sort of system can take into account disturbances which occur after the beginning of a control sequence. Nothing would be lost if a disturbance had not occurred between

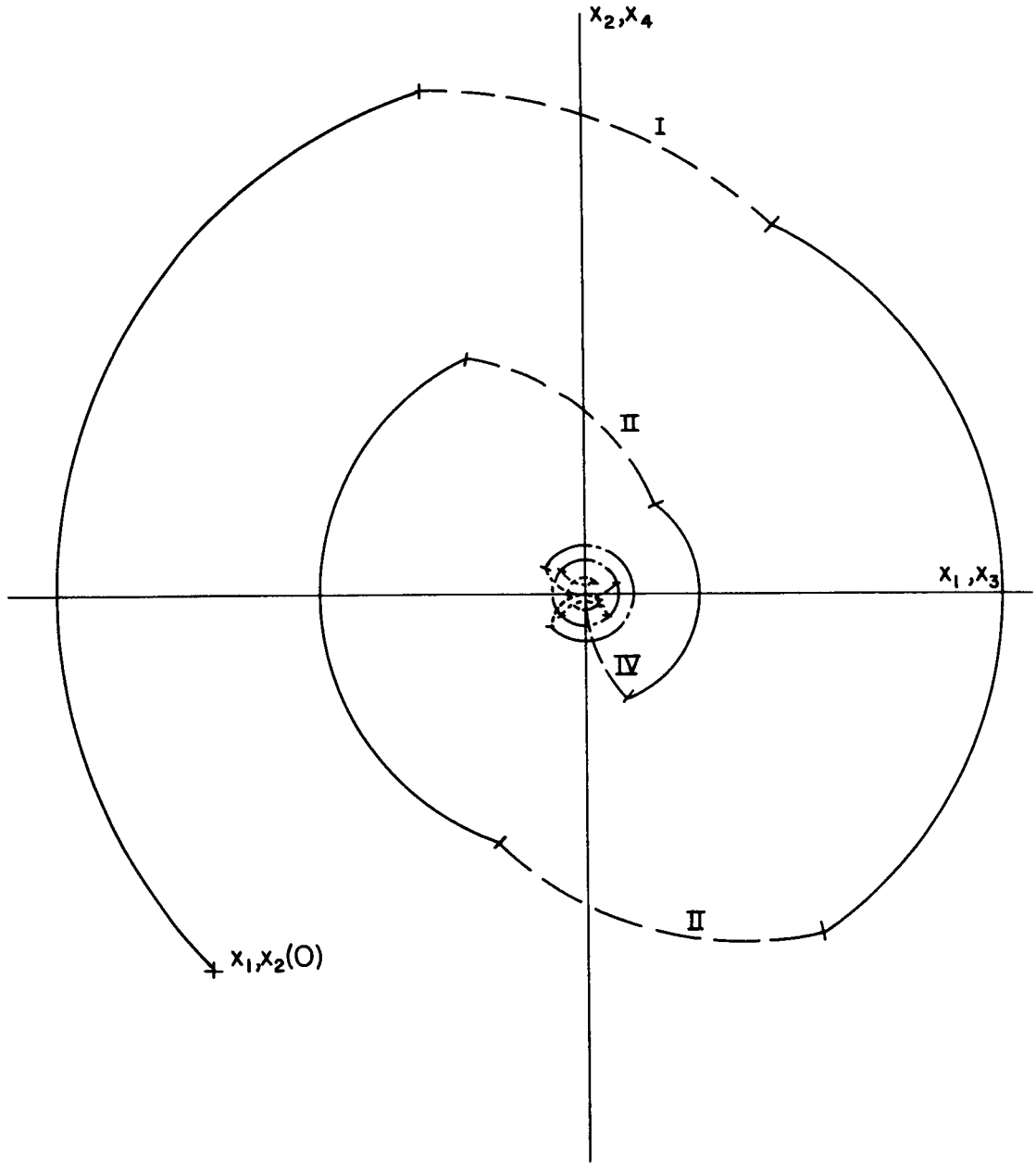

FIG. 32. STATE-SPACE TRAJECTORIES, $\omega_2 = 2.28\ \omega_1$, $X_3(0) = X_4(0) = 0$.

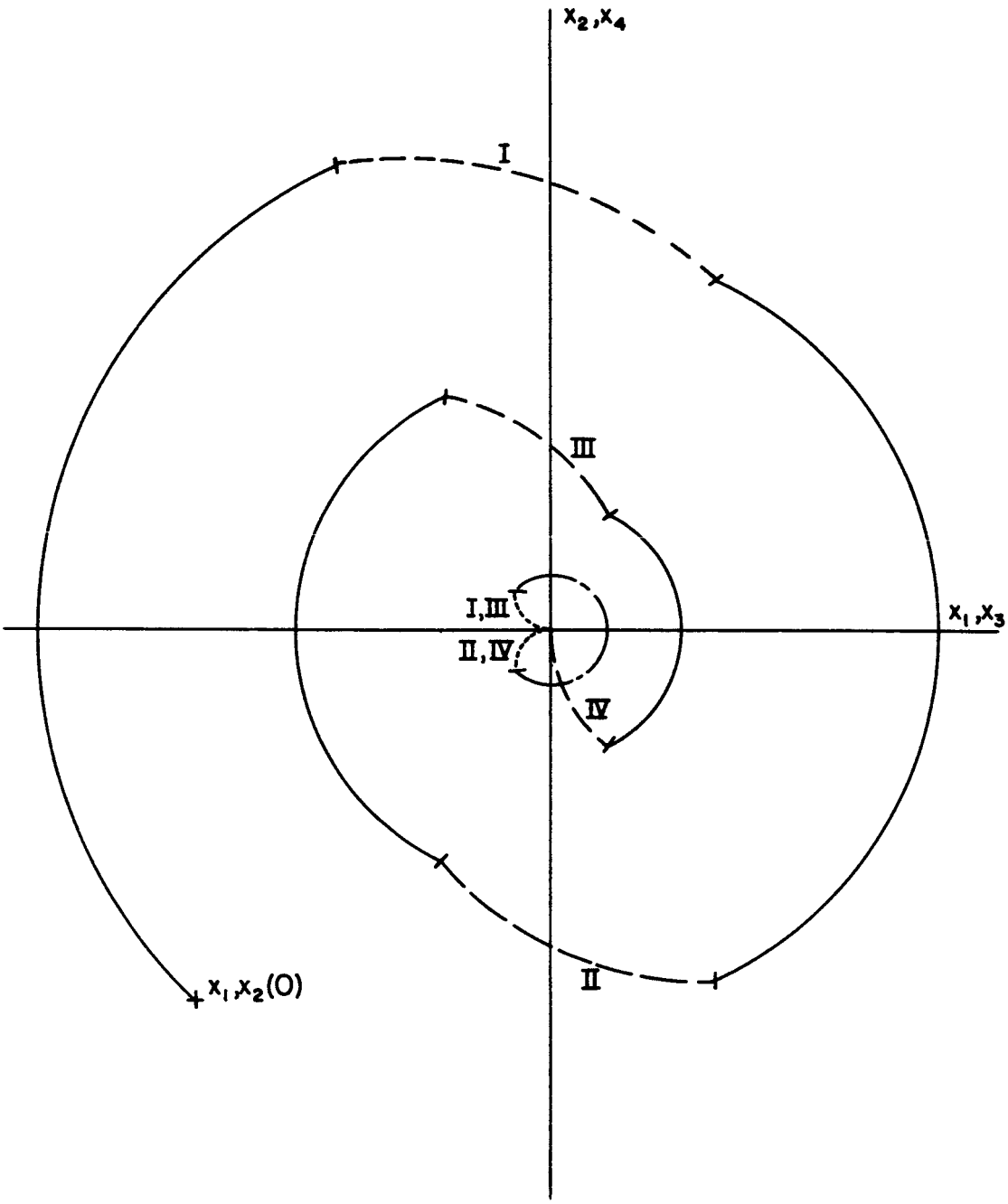

FIG. 33. STATE-SPACE TRAJECTORIES, $\omega_2 = 2.0\ \omega_1$, $X_3(0) = X_4(0) = 0$.

samplings, that is, the amount of fuel expended would not be changed; the recalculated sectors would be identical with those originally established.

An interesting phenomenon takes place if one initial condition is zero and the frequency ratio is an integer value. In Fig. 33, the initial norms were the same as above but ω_2 was changed to be exactly $2\omega_1$. The inner trajectory was actually retraced as the outer trajectory was made to close with the origin, and the sequence of control action was exactly periodic.

The compromise between simplicity of mechanization and satisfactory performance is deemed to be well satisfied by the sub-optimal control. The remaining topic is now generalization of the techniques used here and with the second-order systems.

III. CONCLUSION

To test the general applicability of the techniques of analysis and synthesis which have been used, it might be questioned which of them are unique with either the plant or the control criterion. Of course, observing the behavior of the true optimal control in backward time solutions is a usable technique for any investigation, (excluding systems with inherent chatter (Ref. 2)) so it is mostly a matter of the validity of dealing with the efficiency of control application as a method of approach.

Any oscillatory plant can be put into a form which separates the characteristic modes and these modes can be observed conveniently in $n/2$ state space planes for an n-th order plant. The crux of the matter is, can areas in these $n/2$ planes which simultaneously provide efficient use of a control be used to form an optimal control. Or, in other words, is taking action only in such areas representative of the true optimal control. If this is so, it

amounts to application of a pseudo-superposition rule to a non-linear problem, where rather than say that the optimum for the plant is the sum of the optimums for the separate modes, we say that the optimum action for the plant occurs when the separate optimum actions can be simultaneously satisfied. With this as a heuristic principle, observation of the detailed behavior of the true optimal solutions can guide and correct the development of a realizable control, at least for plants with complex roots.

It is planned to emulate the true optimal control by making the average action of the sub-optimal control equal to the average action of it. Matching the true optimal control element by element means literally solving the two-point boundary value problem, and that is what was set out to avoid. Certainly there are some cases where the exact complete solutions are known in closed form and advantage should be taken of those circumstances, but in general this situation vanishes for plants of order greater than seconds.

As for uniqueness of the cost function, the method of efficiencies was shown to afford some utility for least time as well as least fuel. Minimum error-squared solutions may often closely resemble minimum time solutions and are thus amenable to this technique also.

It is emphasized that the method used does not duplicate the optimal control. To the designer faced with construction of a practical, realizable, control system it does provide an approach to the problem yielding a good compromise answer. More importantly, an insight to the nature of the workings of a true optimal control can be gained quicker with this technique than by wrestling with the complexities of purely mathematical formulation. That is the trait of the scheme which appears to be the most generalizable.

REFERENCES

1. L. S. Pontryagin, V. G. Boltyanskii, R. V. Gamkrelidze, and E. F. Mishchenko,"The Mathematical Theory of Optimal Processes," Interscience Publishers, Inc., New York, N. Y., 1962.

2. A. T. Fuller, "Relay Control Systems Optimized for Various Performance Criteria," Proceedings of IFAC Congress, Moscow, Russia, 1960. Published by Butterworths, London, England, 1962.

3. Cornelius Lanczos, "The Variational Principles of Mechanics," University of Toronto Press, Toronto, 1960.

4. I. Flügge-Lotz and H. Marbach, "The Optimal Control of Linear Systems for a Minimum Control Effort Performance Criterion," SUDAER Report 153, Stanford University, April 1963.

5. I. Flügge-Lotz and H. Marbach, "The Optimal Control of Some Attitude Control Systems for Different Performance Criteria," Journal of Basic Engineering, June 1963, pp. 165-176, ASME Transactions, Vol. 85, Series D.

6. D. B. DeBra, "The Large Attitude Motions and Stability, Due to Gravity, of a Satellite with Passive Damping in an Orbit of Arbitrary Eccentricity About an Oblate Body," SUDAER Report 126, Stanford University, May 1962. (See also Ph.D. thesis, Stanford University, 1962.)

7. J. S. Meditch, "On Minimum-Fuel Satellite Attitude Control," (to be published).

APPENDIX A: RELATIONS $\phi < \frac{\alpha}{2}$

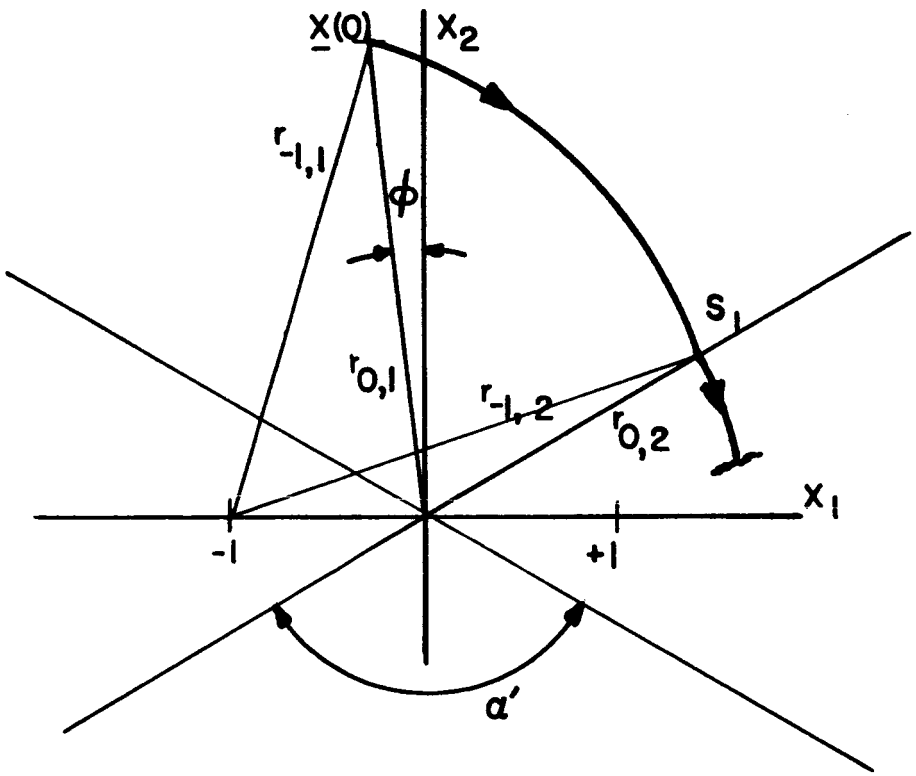

FIG. A-1. TRAJECTORY GEOMETRY.

Again, by the law of cosines,

$$(r_{-1,1})^2 = (r_{0,1})^2 + 1 - 2r_{0,1} \cos(\pi/2 - \phi) \qquad (A.1)$$

$$(r_{-1,2})^2 = (r_{0,2})^2 + 1 - 2r_{0,2} \cos(\pi/2 + \alpha'/2) \qquad (A.2)$$

so

$$(r_{0,1})^2 - (r_{0,2})^2 = 2(r_{0,1} \sin\phi + r_{0,2} \sin\alpha'/2) \qquad (A.3)$$

But $r_{0,2}$ must satisfy Eq. (20), i.e.,

$$\frac{r_{0,2}}{2M} = \sin \frac{\alpha'}{2} \tag{A.4}$$

where $M = N - 1$

Thus, by substituting (A.4) into (A.3) one obtains

$$\left[2(N-1) \sin \frac{\alpha'}{2}\right]^2 = (r_{0,1})^2 - 2r_{0,1} \sin \phi - (2 \sin \frac{\alpha'}{2})(2 \sin \frac{\alpha'}{2})(N-1)$$

$$\left[\sin^2 \left(\frac{\alpha'}{2}\right)\right](4N^2 - 4N) = (r_{0,1})^2 - 2r_{0,1} \sin \phi \tag{A.5}$$

and finally

$$\sin^2 \left(\frac{\alpha'}{2}\right) = \frac{(r_{0,1})^2 - 2r_{0,1} \sin \phi}{4(N^2 - N)} \tag{A.6}$$

Then Eq. (24) yields

$$P_2 = \frac{1}{\cos \frac{\alpha'}{2}} = \frac{1}{\left[1 - \frac{(r_{0,1})^2 - 2r_{0,1} \sin \phi}{4(N^2 - N)}\right]^{1/2}} \tag{A.7}$$

The Eq. (A.6) is singular for the integer $N = 1$. This case requires the zeroing of a disturbance in a single sector when the point lies inside the sector angle. One finds that the admissible initial condition is constrained to a single value,

$$r_{0,1} = 2 \sin \phi$$

and thus is a special case. For other values of the initial point, Eq. (20) is appropriate.

If it is denoted $\underline{X}(0) = r_0 \angle\delta$ and $\underline{p}(0) = f(r_0, \emptyset) \angle\theta$, $f(r_0, \emptyset)$ is given by Eq. (A.7) and θ must be determined.

Unfortunately, phase angle relationships (see Fig. A-2) are not preserved for points within a sector of control action; they are valid only for points on the boundaries of the sector. This can be seen from the following:

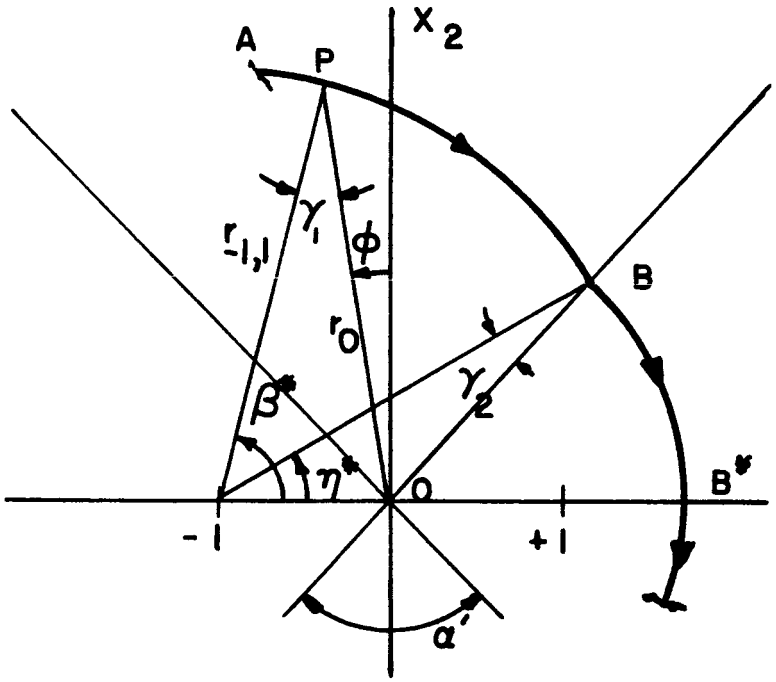

FIG. A-2. TRAJECTORY GEOMETRY.

From triangle (-1, 0, P)

$$\pi = \beta^* + \gamma_1 + \left[(\pi/2) - (\emptyset)\right] \qquad (A.8)$$

From triangle (-1, 0, B)

$$\pi = \eta^* + \gamma_2 + \left[(\alpha'/2) + (\pi/2)\right] \qquad (A.9)$$

Thus

$$\beta^* - \eta^* = \gamma_2 - \gamma_1 + (\alpha'/2) + \phi \qquad (A.10)$$

From Figs. A-2 and 3b, at B^*, $p_2 = 0$. Since $p_2 = P_2 \sin(\omega t + \theta)$, one has

$$(\beta^* - \eta^* + \theta) = (-\pi/2) + (\alpha'/2)$$

Thus

$$\theta = -(\beta^* - \eta^*) - (\pi/2) + (\alpha'/2)$$

or

$$\theta = (\gamma_1 - \gamma_2) - \left[\phi + (\pi/2)\right]$$

$$= (\gamma_1 - \gamma_2) - \delta \qquad (A.11)$$

Let a correction angle $\lambda = \gamma_1 - \gamma_2$ be defined.

From Fig. A-2, and law of cosines one obtains

$$\sin\gamma_2 = \frac{\sin\left[(\pi/2) + (\alpha'/2)\right]}{r_{-1,1}} = \frac{\cos\alpha'/2}{r_{-1,1}} \qquad (A.12)$$

$$\sin\gamma_1 = \frac{\sin\left[(\pi/2) - (\phi)\right]}{r_{-1,1}} = \frac{\cos\phi}{r_{-1,1}} \qquad (A.13)$$

Thus

$$-\lambda = \sin^{-1}\left[\frac{\cos\alpha'/2}{(r_0^2 + 1 - 2r_0\sin\phi)^{1/2}}\right] - \sin^{-1}\left[\frac{\cos\phi}{(r_0^2 + 1 - 2r_0\sin\phi)^{1/2}}\right] \qquad (A.14)$$

λ is smaller than $\alpha'/2$ for all combinations of r_0 and ϕ. The phase angle θ is now given by

$$\theta = -\delta + \left(-\sin^{-1} \left[\frac{\cos \alpha'/2}{(r_0^2 + 1 - 2r_0 \sin \phi)^{1/2}} \right] \right. \tag{A.15}$$

$$\left. + \sin^{-1} \left[\frac{\cos \phi}{(r_0^2 + 1 - 2r_0 \sin \phi)^{1/2}} \right] \right)$$

$\underline{p}(0)$ is determined for an initial condition inside the control sector by Eq. (24), when α is replaced by α'.

APPENDIX B - ANALOG SIMULATION BLOCK DIAGRAM

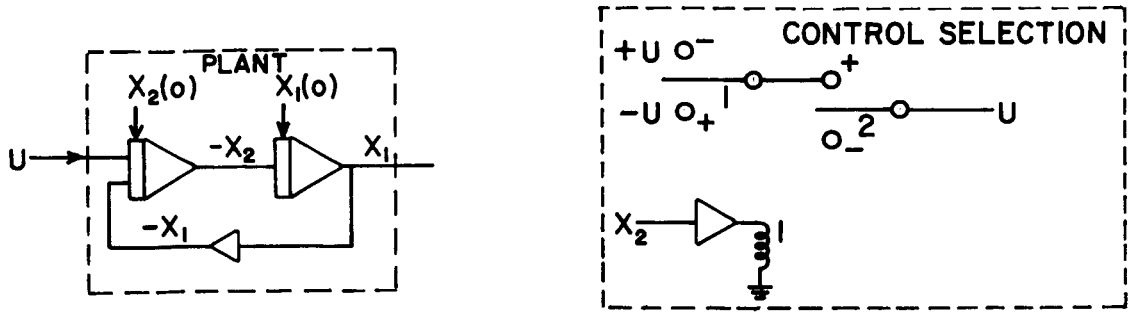

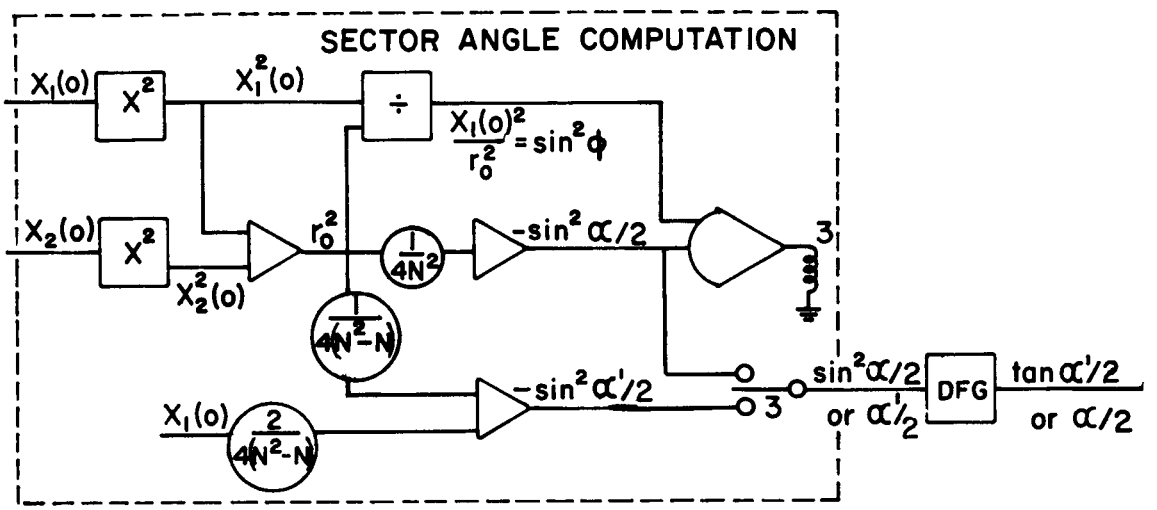

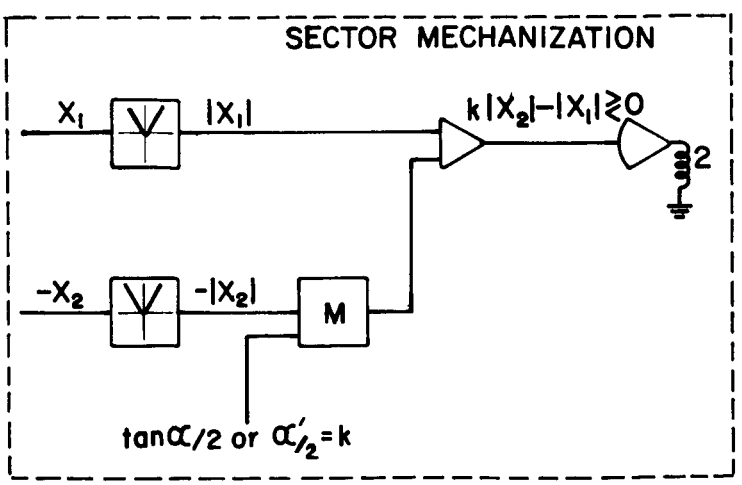

APPENDIX C: MECHANISM OF SWITCHING FOR THE $(1/s^2)$ PLANT

Figure C-1 presents a schematic diagram of the analog computer synthesis for this plant. Each element will be discussed separately:

A) The plant, consisting of two integrations to yield error, X_1.

B) Recognition circuits, whose function it is to determine intersection of the trajectory with one of the parabolae leading to the origin. This is accomplished by having a non-polarized relay (represented by the letters NP inside an amplifier symbol) act upon the sum of two inputs;

$$-(X_1)^2 + 2X_1 \qquad \text{if} \qquad X_1 > 0^*$$

or

$$-(X_1)^2 - 2X_1 \qquad \text{if} \qquad X_1 < 0 .$$

If either of these sums is zero, the relay contacts assume the position marked = 0, while if the magnitude of the sum is not equal to zero, the contact labeled $\neq 0$ is connected to the armature. (These points correspond to β and α in the "Control Selection" block.)

Since only the upper half of the left-opening parabola and the lower half of the right-opening are the desired paths to recognize, generation of two types of control, α and β , are necessary as will be explained in the "Quadrant Determination" section.

---

*Switching for the correct one of the two possible equations is accomplished by the polarized relay marked 2, Fig. C-1.

C) Quadrant Determination, both with regard to selection of when to shut off the fuel - i.e., quadrant determination of biased horizontal axes - as well as upper and lower half parabola determination. These conditions are satisfied by a logic table: Let U_{max} = 20 volts, then to satisfy the control laws;

Quadrant	1	2	3	4
α =	-20	0	+20	0
β =	0	+20	0	-20

It should be noted that the α quadrant determination is a biased quadrant determination, and that the bias voltage polarity must be altered when X_1 changes sign, as provided for by the (10 sgn X_1) input to the bias potentiometer B.

D) Control selection, simply selecting α until intersection with a parabola through the origin whereupon β is chosen.

An illustrative example will demonstrate how the mechanism works. Taking an initial point in the first quadrant, α = -20 while β = 0. Since there is no desired half-parabola to the origin in the first quadrant, α is selected (the sum of the inputs to the non-polarized relay is not zero). As the trajectory crosses the horizontal axis and enters the 2nd quadrant, at some value of X_2 - namely the bias value - α will change to zero thereby causing the trajectory to commence a horizontal path toward the X_2 axis. It will continue this path until it intersects the half-parabola whereupon the control will switch to β, which is +20 in this quadrant. This will continue in force until a dead zone is reached in the vicinity of the origin, if one has been implemented, or a chatter results.

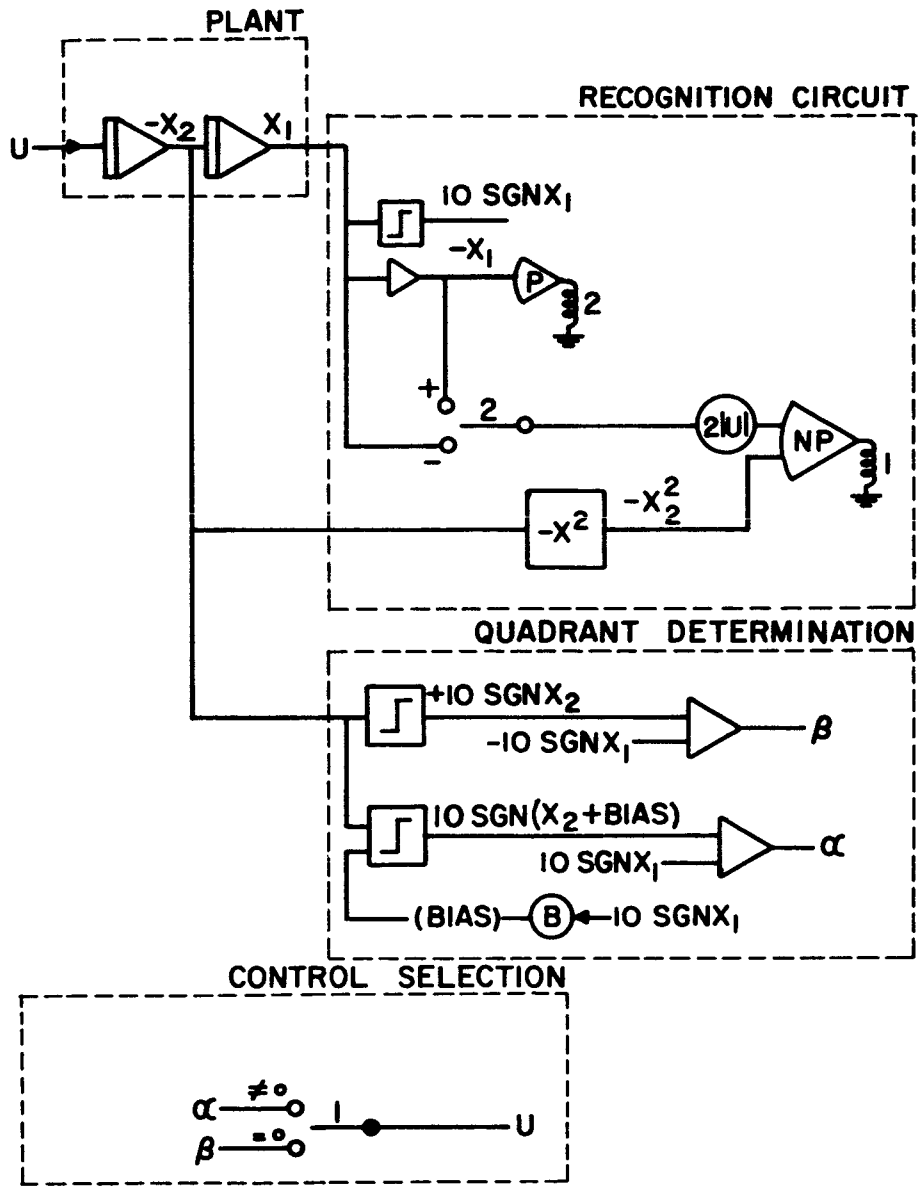

FIG. C-1. ANALOG SIMULATION BLOCK DIAGRAM.

APPENDIX D: LINEAR TRANSFORMATION RELATIONS

The matrix B is given by

$$B = \begin{bmatrix} \frac{\alpha_1}{\omega_1} & 0 & 0 & \frac{\omega_1(\omega_2^2 - 4\alpha_2)}{4\alpha_2(1 - \alpha_2)} \\ 0 & 1 & \frac{4\alpha_2 - \omega_2^2}{1 - \alpha_2} & 0 \\ 0 & \frac{\omega_2(\alpha_1 - \omega_1^2)}{\alpha_1(1 - \alpha_1)} & \frac{4\alpha_2}{\omega_2} & 0 \\ \frac{\omega_1^2 - \alpha_1}{1 - \alpha_1} & 0 & 0 & 1 \end{bmatrix}$$

ω_1 and ω_2 are the roots of the equation

$$s^4 + \left[(1 - \alpha_1)(1 - \alpha_2) + \alpha_1 + 4\alpha_2\right] s^2 + 4\alpha_1\alpha_2 = 0$$

The coupling coefficients are given by

$$\beta_1 = \frac{\omega_1 (4\alpha_2 - \omega_2^2)}{4\alpha_2 (\alpha_2 - 1)}$$

$$\beta_2 = \frac{\omega_2 (\alpha_1 - \omega_1^2)}{\alpha_1 (1 - \alpha_1)}$$

APPENDIX E - TRUE OPTIMAL SIMULATION.

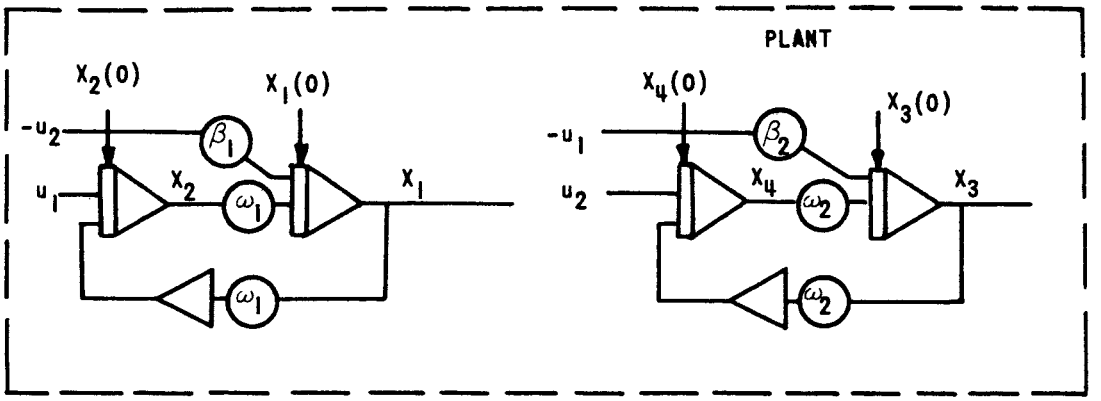

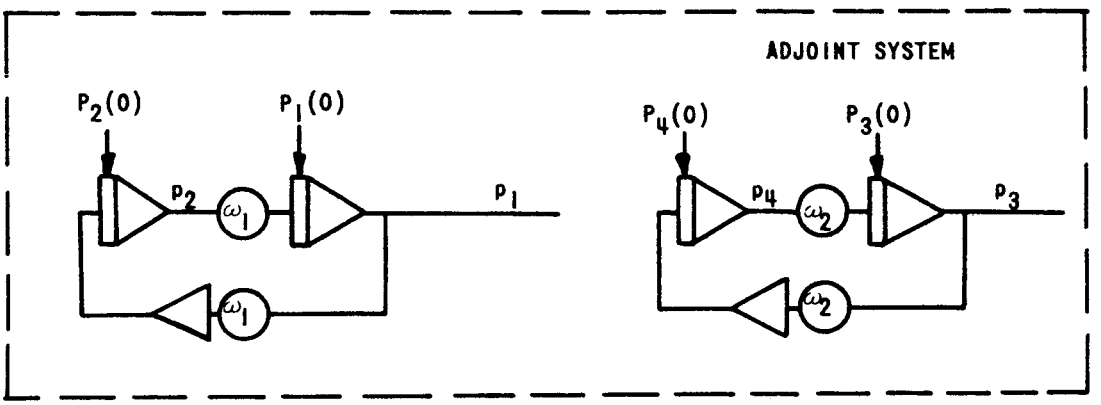

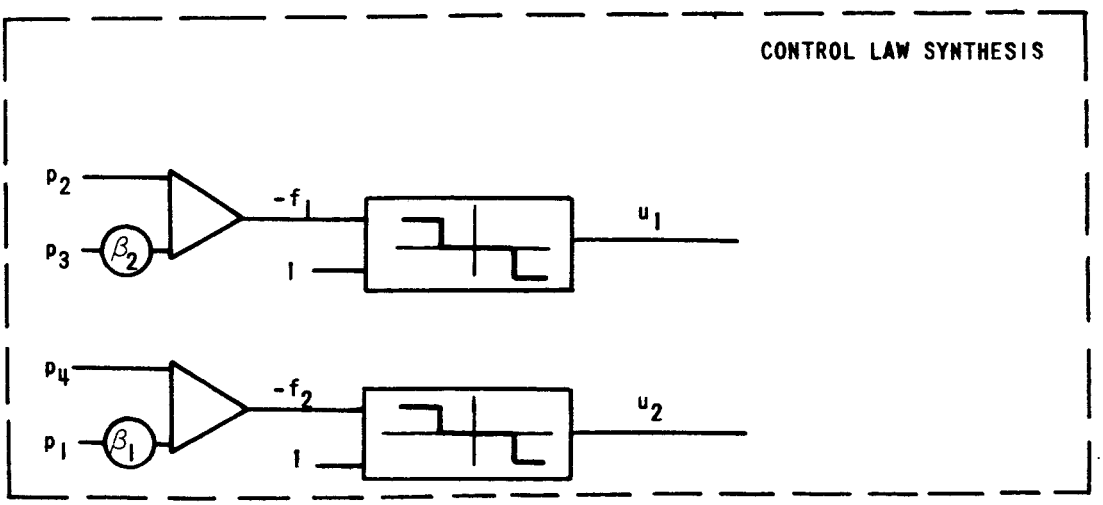

APPENDIX F - TRUE OPTIMAL SIMULATION
PERFORMANCE DATA.

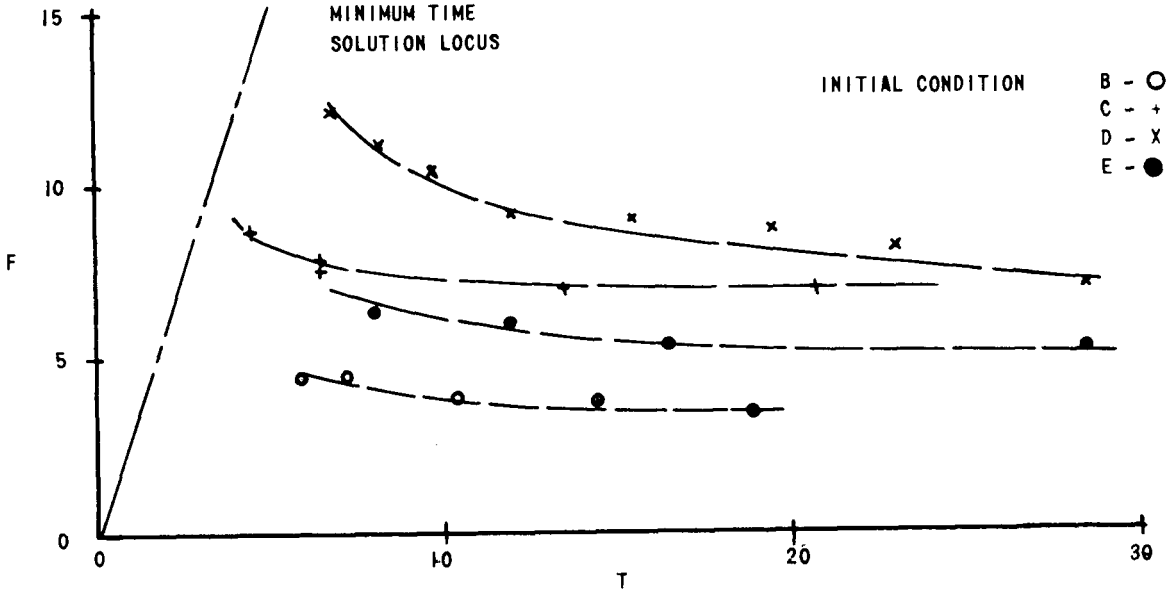

FIG. F-1. FUEL USAGE VS TIME FOR SOLUTION.

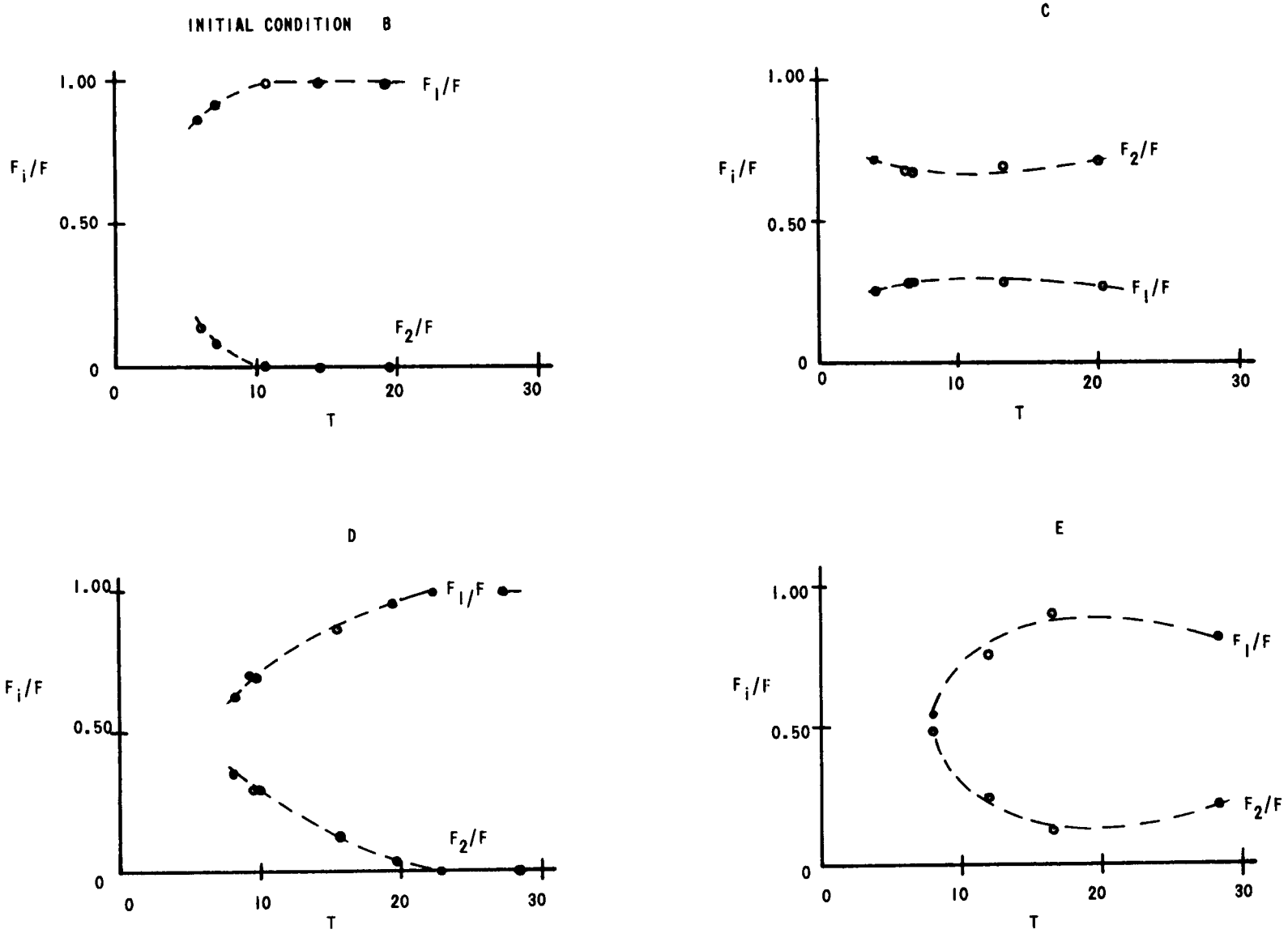

FIG. F-2. FUEL APPORTIONMENT.

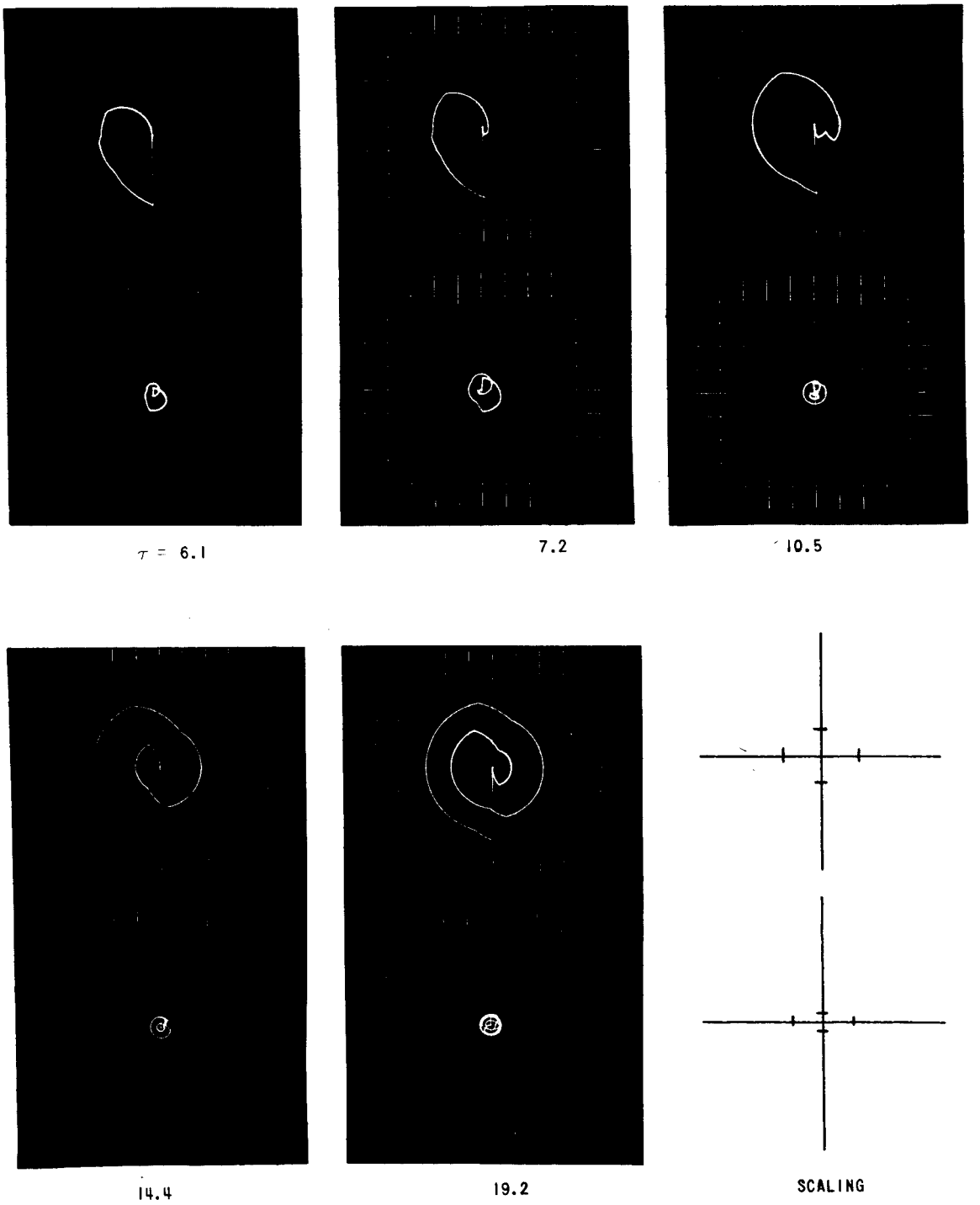

FIG. F-3 FAMILY OF TRUE OPTIMAL SOLUTIONS.

APPENDIX G: PHASE ANGLE RELATIONS

For the geometry of the figure below

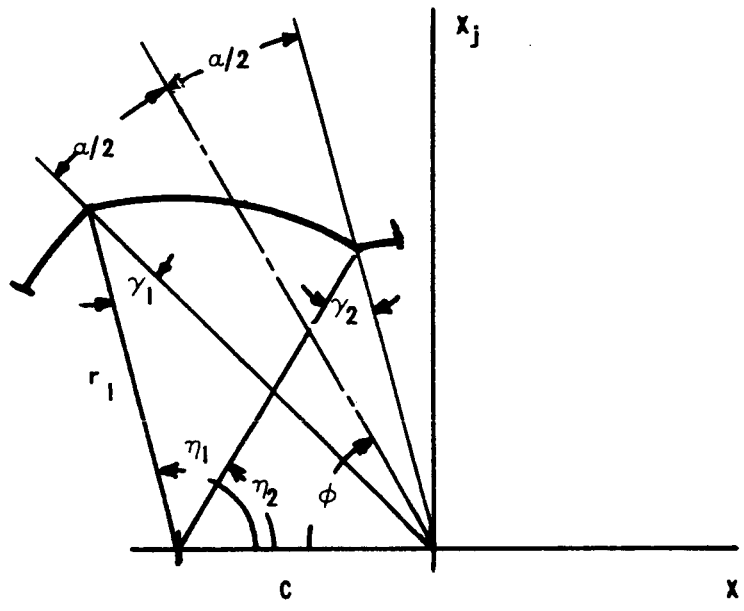

$$\eta_1 + \gamma_1 + (\phi - \frac{\alpha}{2}) = \eta_2 + \gamma_2 + (\phi + \frac{\alpha}{2}) \qquad \text{(G-1)}$$

$$\Delta\eta = \eta_1 - \eta_2 = (\gamma_2 - \gamma_1) + \alpha \qquad \text{(G-2)}$$

$\frac{\Delta\eta}{\omega}$ = Duration of control application

α = Change in state space phase angle

From law of sines,

$$\frac{r_1}{\sin(\phi - \alpha/2)} = \frac{C}{\sin\gamma_1} \qquad \text{(G-3)}$$

and

$$\frac{r_1}{\sin(\phi + \alpha/2)} = \frac{C}{\sin\gamma_2} \qquad \text{(G-4)}$$

Solving for $\sin \gamma_2$ and $\sin \gamma_1$, the difference can be written:

$$\sin \gamma_2 - \sin \gamma_1 = \frac{C}{r_1} \left[\sin(\phi + \alpha/2) - \sin(\phi - \alpha/2)\right]$$

$$= \frac{C}{r_1} 2 \cos \phi \sin \alpha/2 \qquad \text{(G-5)}$$

In the region of interest,

$$\frac{C}{r_1} < 1 \quad \text{and} \quad 0 < \alpha < 2\pi \quad ,$$

so that if $\phi < \pi/2$,

$$\sin \gamma_2 > \sin \gamma_1 \; ;$$

$$\text{thus } (\gamma_2 - \gamma_1) > 0$$

$$\text{and } \Delta\eta > \alpha \, .$$

If $\phi > \pi/2$,

$$\sin \gamma_1 > \sin \gamma_2 \, ,$$

$$\Delta\eta < \alpha \, .$$

Thus the state-space phase angle is altered in time by an amount less than or greater than the amount (ω)(duration of control application), depending on the orientation of the sector of application. The two angles are equal only for control application symmetric about the maximum action line.

APPENDIX H: SCALING OF STATE VARIABLES

A realistic level of error signal in angular velocity for a gravity-gradient stabilized vehicle like the Agena* is 0.02 degrees/second. Converting to dimensionless time,

$$\overset{o}{\Psi} = \frac{1}{n} \dot{\Psi}$$

A typical orbital period is 90 minutes, so that $n = 2\pi /(90)(60)$ rad/sec. Thus

$$\overset{o}{\Psi} = \frac{(90)(60)}{2\pi} \left(\frac{.02}{57.2}\right) = 0.3$$

That value was chosen for $\underline{R}(0)$ for runs C and D in Table II.

Substitution of the parameter values into the matrix B results in this relationship between $\underline{X}$ and (Ψ, Φ)

$$\underline{X} = \begin{bmatrix} 0.75 & 0 & 0 & 0.23 \\ 0 & 1 & -.70 & 0 \\ 0 & 0.40 & 1.31 & 0 \\ -0.11 & 0 & 0 & 1 \end{bmatrix} \begin{vmatrix} \Psi \\ \overset{o}{\Psi} \\ \Phi \\ \overset{o}{\Phi} \end{vmatrix}$$

so that X_2 is of the order of $\overset{o}{\Psi}$ and $\underline{X}_4$ is of the order of $\overset{o}{\Phi}$

*Data courtesy of D. B. DeBra, Ref. 6.